Ecological Informatics 75 (2023) 102056

Contents lists available at ScienceDirect

Ecological Informatics

journal homepage: www.elsevier.com/locate/ecolinf

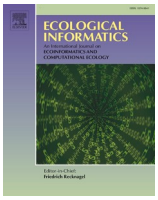

A dynamic integrated model for mercury bioaccumulation in marine organisms

Giovanni Denaro [a,b,c], Luciano Curcio [c,d], Alessandro Borri [e,f,*], Laura D'Orsi [e], Andrea De Gaetano [c,e,g]

[a] Laboratory of Ecology, Department of Earth and Marine Sciences, University of Palermo, Viale delle Scienze Edificio 16, I-90128 Palermo, Italy
[b] NBFC, National Biodiversity Future Center, Piazza Marina 61, I-90133 Palermo, Italy
[c] National Research Council of Italy - Institute for Biomedical Research and Innovation (IRIB-CNR), Via Ugo La Malfa 153, I-90146 Palermo, Italy
[d] Department of earth and marine science (DiSTeM), University of Palermo, I-90128 Palermo, Italy
[e] National Research Council of Italy - Institute for Systems Analysis and Computer Science "A. Ruberti" (IASI-CNR), I-00168 Rome, Italy, I-67100, L'Aquila, Italy
[f] Center of Excellence for Research DEWS, University of L'Aquila, Via Vetoio Coppito 1, I-67100 L'Aquila, Italy
[g] Dept. of Biomatics, Obuda University, Budapest, Hungary

ARTICLE INFO

Keywords:
Dynamic model
Marine ecology
Ordinary differential equations
Mercury dynamics

ABSTRACT

A novel integrated dynamic model, the Integrated Fish Model (INTFISH), incorporating mercury (Hg) dynamics at non-steady state in marine organisms, is presented and is applied to the benthic food web in a polluted area. The integrated Fish model represents the dynamics of inorganic mercury (Hg^{II}) and methyl-mercury (MeHg) in a real marine ecosystem including environmental (seawater and sediments) and biota compartments. Mercury concentration in fish is estimated using the INTFISH model coupled, in real-time, with results from i) the seawater and sediments modules computed using the HR3DHG model, ii) a dedicated Phytoplankton model and iii) six modules for Hg fluxes within the invertebrate compartment, incorporating the main organisms included in fish diet preferences, whose variations during the whole life cycle are also taken into account to verify the sensitivity of the integrated model to the core set of parameters. The simulated total mercury concentrations (Hg^{TOT}) in specimens of red mullet (*Mullus barbatus*), selected as target species for the Fish model, are in excellent agreement with field observations reported from the investigated area. The intrinsic modularity of the model offers the opportunity to extend simulations to other fish species (which are part of the diet of human populations of interest) and predict Hg concentration in food. A natural extension of the model will allow to evaluate the health risks related to human consumption of contaminated fish.

1. Introduction

The description and evaluation of the consequences of toxic chemical accumulation in ecosystems (soil, air, water, plants, animals and humans) certainly play a key role in environmental risk assessment in particular polluted areas (Kaikkonen et al., 2020; Sadutto et al., 2021; Senthil Rathi et al., 2021; Van der Oost et al., 2003; Visha et al., 2021). In particular, great attention is paid to water pollution, since water covers most of our planet (70%). Many toxicants interact with the aquatic habitat in general and, especially in seas and oceans, pollution depends on the spillage of man-made products such as pesticides, herbicides, fertilizers, detergents, oil, industrial chemicals and wastewater (He et al., 2012).

One of the most harmful chemical contaminants for humans is certainly mercury and understanding the mechanisms regulating its accumulation in the marine food web has become, over the past few years, one of the most urgent challenges in the field of toxicokinetics of heavy metals (Bieser and Schrum, 2016; Booth and Zeller, 2005; Fitzgerald et al., 2007; Gworek et al., 2016; Hylander and Goodsite, 2006; Jagadeep et al., 2020; Kütter et al., 2009; Ni et al., 2017). The exposure to methyl-mercury (MeHg), the most toxic mercury species, is reported to cause irreversible damages to the central nervous system (Carrier et al., 2001; De Flora et al., 1994; Mergler et al., 2007; Storelli et al., 2003), as well as teratogenic effects in the foetus during the embryonic

* Corresponding author at: National Research Council of Italy, Institute for Systems Analysis and Computer Science "A. Ruberti" (IASI-CNR), UCSC Largo A. Gemelli 8, I-00168, Rome, Italy.
E-mail address: alessandro.borri@iasi.cnr.it (A. Borri).

https://doi.org/10.1016/j.ecoinf.2023.102056
Received 25 July 2022; Received in revised form 28 December 2022; Accepted 1 March 2023
Available online 21 March 2023

phase (Brender et al., 2006; Jin et al., 2016; Matsumoto et al., 1965). Furthermore, MeHg biomagnifies in marine food webs, resulting in higher concentrations in upper trophic level marine species with respect to their prey (Harding et al., 2018; Johnsson et al., 2005; La Colla et al., 2019; Lee and Fisher, 2017; Li et al., 2022; Mackay and Fraser, 2000; Marziali et al., 2021; Morcillo et al., 2017; Signa et al., 2017).

On top of that, the marine-coastal areas have undergone a significant anthropogenic impact over the years as happened for the Augusta Bay, in Sicily, which has been one of the most polluted marine areas in Italy because, since 1950, petrochemical plants-derived pollution has been entering water at this site (Bagnato et al., 2013; Bellucci et al., 2012; Salvagio Manta et al., 2016; Sprovieri et al., 2011). Mercury, in particular, is one of the main pollutants in this area, because of the discharges of large mercury-cell chlor-alkali plants operative until 1970s (Bellucci et al., 2012; Le Donne and Ciafani, 2008).

Several experimental investigations in the area demonstrated an active transfer of mercury from the abiotic compartment (seawater and sediments) to marine organisms (Ausili et al., 2008; Bonsignore et al., 2015; ICRAM, 2008; Oliveri et al., 2016; Salvagio Manta et al., 2016) and highlighted serious risks for human health due to consumption of seafood from that area (Bonsignore et al., 2013, 2016; Di Bella et al., 2020).

Over the last decades, several theoretical studies introduced innovative tools to describe both the migration mechanisms of inorganic and organic pollutants from the abiotic aquatic ecosystems to organisms and transfer from prey to predator along the food webs (Connell, 1990; Sharpe and Mackay, 2000). Specifically, bioaccumulation models that exploit ordinary differential equations (ODE) have been used to reproduce effects of pollutant bioaccumulation and biodilution. Initially, simple equilibrium partitioning models, based on the octanol-water partition coefficient (K_{ow}) and the bioconcentration factor (BCF), have been proposed for several classes of organic pollutants (Arnot and Gobas, 2004; Hamelink et al., 1971; Neely et al., 1974; Veith et al., 1979). Kinetic models have been developed to reproduce at the steady state the distribution of chemicals in each trophic level of the aquatic food web (Clark et al., 1990; Connolly and Tonelli, 1985; Thomann, 1981; Thomann, 1989; Thomann and Connolly, 1984). Then, starting with kinetic models, fugacity-based models (or thermodynamic models) were developed to simulate, at steady state, the bioconcentration and biomagnification process of pollutant transfer along the food webs from contaminated water and sediment (Mackay, 1982; Gobas and MacKay, 1987; Clark et al., 1990; Campfens and Mackay, 1997; Arnot and Gobas, 2004). In the 1990s, for the first time, Hendriks modified the fugacity theory to develop the kinetic models at non-steady state, models in which rate constants for influx and efflux were defined, for each trophic level, as a function of i) pollutant concentration in the environment and ii) weight of the investigated organism (Hendriks, 1995, 1999; Hendriks et al., 2001; Hendriks and Heikens, 2001). Based on this approach, innovative bioaccumulation models for marine species (named Phytoplankton model, Invertebrate model, Fish model) have recently been introduced in the MERLIN-Expo library (https://merlin-expo.eu/). In this ensemble of models, the dynamics of the contaminant concentration in the body of each organism is reproduced, excluding migration of marine species (Radomyski and Ciffroy, 2015a, 2015b, 2015c). Although this assumption can be acceptable for most of phytoplankton and invertebrate species, it appears ineffective for fish species which migrate during their life cycle. Physiologically based pharmacokinetic (PBPK) models for chemicals bioaccumulation in fish have been developed since the early 1990s (Arnot and Gobas, 2004; Law et al., 1991; Nichols et al., 1990) but, being multi-compartmental, they need substantial experimental datasets to be calibrated and validated.

In this work, we introduce the Integrated Fish Model, INTFISH, which has been designed and implemented to reproduce, in non-equilibrium conditions, the dynamics of total mercury (Hg^{TOT}) concentration in a target fish species (*Mullus barbatus*) during its whole life cycle. The kinetic model never reaches a stationary state, since the mercury concentrations from the source biogeochemical model (Denaro et al., 2020) change as a function of time and space position, causing the variations in Hg concentration in each trophic level. INTFISH consists of i) a Fish Model, coupled in real time with ii) the seawater and sediments modules of HR3DHG (Denaro et al., 2020), iii) the Phytoplankton Model (Hendriks and Heikens, 2001; Radomyski and Ciffroy, 2015a) and iv) six modules of the Invertebrate Model (Hendriks and Heikens, 2001; Radomyski and Ciffroy, 2015b), applied to a single species, characterising dietary preference. The model frame was chosen based on the food web structure, which affects mercury transfer from one trophic level to another (Lee and Fisher, 2017). Due to different toxicity and bioaccumulation, the dynamics of Hg^{II} and MeHg in the marine organisms were analyzed separately. In this way, the bioaccumulation processes for both Hg species are reproduced by considering all mercury fluxes exchanged from phytoplankton (trophic level 1) to fish (level trophic 3), passing through the intermediate trophic level, i.e. invertebrates. INTFISH is calibrated and validated using previous experimental data collected in Augusta Bay, southern Italy (Bonsignore et al., 2013; Di Bella et al., 2020).

To the best of our knowledge, this is the first time that an integrated mathematical model is designed to quantify the time course of toxicant concentration in marine organisms, i) by assuming as input to the system the transient behaviour obtained by a coupled spatio-temporal high-resolution model (HR3DHG), which in turn accounts for seasonal environmental variability; ii) by considering bioaccumulation and mercury transfer along the whole food web of a target fish species with possibly time-varying dietary habits; iii) by proposing a modular framework which can be easily adapted to fit experimental data possibly related to different locations and species with respect to those considered in this work.

2. Material and methods

2.1. Mercury bioaccumulation modelling: a synthetic view

The INTFISH model has been designed and implemented to reproduce the dynamics of Hg^{TOT} (Hg^{II}_{fish} and $MeHg_{fish}$) during all stages of fish life cycle, following the diet preferences of both the red mullet (*M. barbatus*) and its prey. Bioaccumulation processes are therefore simulated considering all mercury fluxes exchanged throughout the overall food web. The model results are then compared with the Hg^{TOT} concentration in fish at the time of capture, as reported by Bonsignore et al. (2013) and Di Bella et al. (2020).

The main module of INTFISH is the Fish Model, which is coupled, in real-time, with the seawater module of HR3DHG Model (Denaro et al., 2020) and with six modules of the kinetic model for invertebrates (the Invertebrate Model), one for each fish diet preference. The HR3DHG Model provides the inputs for the fish respiratory system, i.e. Hg^{II} and MeHg concentration in seawater, while the Invertebrate modules give the inputs for its gastro-intestinal tract (GIT), i.e. the Hg^{II} and MeHg concentration in the main prey (Hg^{II}_{j} and $MeHg_{j}$). Each Invertebrate module is also integrated in real-time with the seawater and sediment modules of HR3DHG Model (Hg^{II}_{sed} and $MeHg_{sed}$), the kinetic model for phytoplankton (Phytoplankton model – Hg^{II}_{phy} and $MeHg_{phy}$) and the other Invertebrate modules (Fig. 1).

Since the *M. barbatus* feeds on prey living in the seabed of coastal areas, the mercury concentrations in phytoplankton and invertebrates are calculated at each node (x, y) of the same 2D grid used in the HR3DHG Model for the sediment surface layer of Augusta Bay.

2.2. Phytoplankton model

The Phytoplankton Model (Eqs. (1)–(5)) is a kinetic model and provides the dynamics of mercury concentrations in picoeukaryotes, i.e. the most representative phytoplankton population in terms of biomass (Hendriks and Heikens, 2001; Radomyski and Ciffroy, 2015a) in the

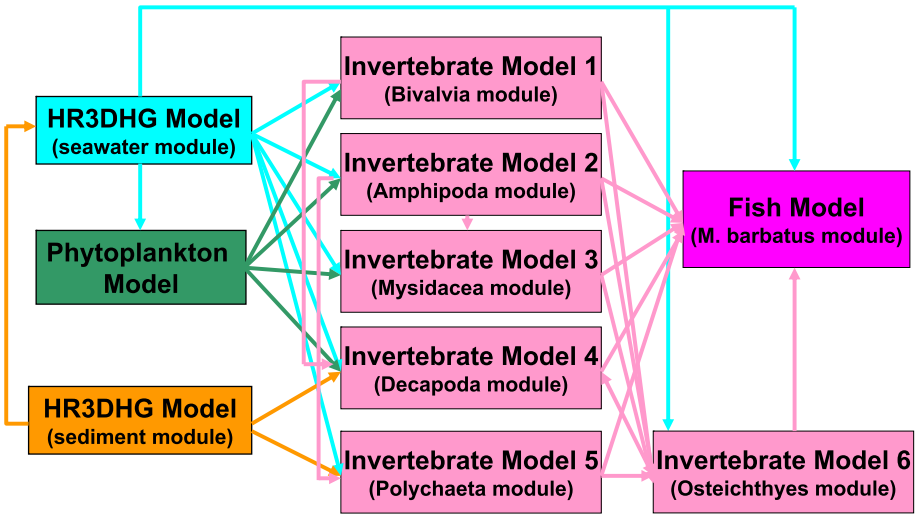

Fig. 1. Basic scheme of the Integrated Fish Model: the main block is the Fish Model (fuchsia colour box), other blocks are six Invertebrate Models (pink box) and the Phytoplankton Model (green box). The seawater module (light blue box) of HR3GHG Model provides input for all modules of the Integrated Fish Model; the HR3GHG Model sediment module (orange box) instead, communicates only with some modules of the Invertebrate Model. (For interpretation of the references to colour in this figure legend, the reader is referred to the web version of this article).

Mediterranean Sea (Brunet et al., 2006, 2007). More generally, picoplankton has been shown to contribute greatly to the biomass of food webs in both marine and freshwater ecosystems (Likens, 2009), where they are often responsible for most of the marine primary production (Stockner and Antia, 1986), providing energy to higher trophic levels (Schmidt, 2019).

In our modelling framework, the Phytoplankton Model provides estimates of mercury deriving from phytoplankton accumulation and absorbed, via the gastro-intestinal tract (GIT), by amphipoda, mysidacea, decapoda and bivalvia (Invertebrate Model 1 – Invertebrate Model 4).

The mercury contents in phytoplankton strongly depend on the concentrations of the respective mercury species (Hg^{II} and *MeHg*) dissolved in seawater and absorbed by phytoplankton through its cellular membrane. It is modelled considering three biological processes (Hendriks and Heikens, 2001; Radomyski and Ciffroy, 2015a):

i) absorption of the two mercury species through the phytoplankton cell membrane (uptake term);
ii) excretion of the two mercury species through the phytoplankton cell membrane (excretion term);
iii) excretion of the two mercury species for dilution through the size growth of phytoplankton cell (growth term).

Thus, the kinetic model for the mercury concentrations in phytoplankton biomass is defined by the following ordinary differential equations:

$$\frac{dHg^{II}_{phy}}{dt} = k_{phy,up\_ino}\cdot\left[Hg^{II}\right] - Hg^{II}_{phy}\cdot\left(k_{phy,exc_{ino}} + k_{phy,gr}\right) \quad (1)$$

$$\frac{dMeHg_{phy}}{dt} = k_{phy,up\_met}\cdot[MeHg] - MeHg_{phy}\cdot\left(k_{phy,exc\_met} + k_{phy,gr}\right) \quad (2)$$

where

- Hg^{II}_{phy} and $MeHg_{phy}$ are the Hg^{II} and MeHg concentrations in phytoplankton biomass, respectively $[\mu g\cdot kg^{-1}_{wet\_wt}]$;
- $k_{phy,\ up\_ino}$ and $k_{phy,\ up\_met}$ are the rate constants for the uptake from the seawater of IHg and MeHg, respectively $[l\cdot kg^{-1}_{wet\_wt}\cdot d^{-1}]$;
- $[Hg^{II}]$ and $[MeHg]$ are the concentrations of IHg and MeHg in seawater, respectively $[\mu g\cdot l^{-1}]$;
- $k_{phy,\ exc\_ino}$ and $k_{phy,\ exc\_met}$ are the rate constants for the excretion with seawater of IHg and MeHg, respectively $[d^{-1}]$;
- $k_{phy,\ gr}$ is the dilution rate constant associated with phytoplankton biomass growth $[d^{-1}]$.

The rate constants are defined as follows:

$$k_{w,ino,up} = \frac{W^{-\kappa}_{phy}}{\rho_w + \rho_{lip,in}\cdot[Hg^{II}]^{\kappa^{II}_p} + \frac{1}{\gamma_0}};\ k_{w,met,up} = \frac{W^{-\kappa}_{phy}}{\rho_w + \rho_{lip,in}\cdot[MeHg]^{\kappa^{MM}_p} + \frac{1}{\gamma_0}} \quad (3)$$

$$k_{w,ino,exc} = \frac{1}{K^{II}_{tw}\cdot p_{s,phy}}\cdot\frac{W^{-\kappa}_{phy}}{\rho_w + \rho_{lip,out} + \frac{1}{\gamma_0}};\ k_{w,met,exc} = \frac{1}{K^{MM}_{tw}\cdot p_{s,phy}}\cdot\frac{W^{-\kappa}_{phy}}{\rho_{w,phy} + \rho_{lip,out} + \frac{1}{\gamma_0}} \quad (4)$$

$$k_{phy,gr} = q_T\cdot\gamma_2\cdot W^{-\kappa}_{phy} \quad (5)$$

where

- W_{phy} *is the average phytoplankton cell weight* $[kg_{wet\_w}]$;
- κ is the rate exponent [dimensionless];
- ρ_w is the water layer diffusion resistance $[d\cdot kg^{-\kappa}]$;
- $\rho_{lip,\ in}$ is the lipid layer permeation influx resistance $[d\cdot kg^{-\kappa}\cdot\mu g^{-\kappa_p}\cdot l^{\kappa_p}]$;
- κ^{II}_p and κ^{MM}_p are the lipid resistance exponents for IHg and MeHg, respectively [dimensionless];
- γ_0 is the water absorption-excretion coefficient $[kg^{\kappa}\cdot d^{-1}]$;
- K^{II}_{tw} and K^{MM}_{tw} are the dry tissue-water partition ratios for IHg and MeHg, respectively $[kg^{-1}_{dry\_wt}/l^{-1}]$;
- $p_{s,\ phy}$ is the dry fraction of phytoplankton $[kg_{dry\_wt}/kg_{wet\_wt}]$;
- $\rho_{lip,\ out}$ is *the* lipid layer permeation efflux resistance $[d\cdot kg^{-\kappa}]$;
- q_T is the *temperature* correction factor [dimensionless]; γ_2 is the biomass reproduction coefficient $[kg^{\kappa}\cdot d^{-1}]$.

The parameters used, obtained according to available literature (Hendriks et al., 2001; Hendriks and Heikens, 2001) are reported in Table 1. The *average phytoplankton cell weight* (W_{phy}) is calculated by the average phytoplankton cell volume using the method of Radomyski and Ciffroy (2015a). Assuming that the most representative phytoplankton population in terms of biomass is that of picoeukaryotes (Brunet et al., 2006, 2007), their average cell volume (Strickland, 1960) is used to obtain the average phytoplankton cell weight.

2.3. Invertebrate model

The dynamics of mercury in the prey categories of fish is reproduced using the kinetic model devised for invertebrates, i.e. the Invertebrate Model (Hendriks and Heikens, 2001; Radomyski and Ciffroy, 2015b). In general, Hg concentrations in the considered prey (invertebrates) strongly depend on mercury concentrations in the ingested marine organisms (phytoplankton, zoobenthos, etc.) and the assimilated detritus,

Table 1
Biological parameters used in the Integrated Fish Model.

Symbol	Interpretation	Unit	Value	Reference
W_{phy}	Average phytoplankton cell weight	kg	$14*10^{-15}$	Strickland (1960)
W_{biv}	Average weight of bivalvia	kg	$4.3*10^{-3}$	Radomyski and Ciffroy (2015b)
W_{amp}	Average weight of amphipoda	kg	$38*10^{-6}$	McKinney et al. (2004)
W_{mys}	Average weight of mysidacea	kg	$1.0*10^{-4}$	Campfens and Mackay (1997)
W_{dec}	Average weight of decapoda	kg	$133*10^{-4}$	McKinney et al. (2004)
W_{pol}	Average weight of polychaeta	kg	$162*10^{-6}$	Yakovlev and Yakovleva (2010)
W_{ost}	Average weight of osteichthyes	kg	$16*10^{-3}$	Campfens and Mackay (1997)
κ	Rate exponent	dimensionless	0.25	Hendriks et al. (2001)
ρ_w	Water layer diffusion resistance	d $kg^{-\kappa}$	0.0028	Hendriks et al. (2001)
$\rho_{w,ege}$	Water layer diffusion resistance for assimilation of chemicals from food	d $kg^{-\kappa}$	0.000011	Hendriks et al. (2001)
$\rho_{lip,in}$	Lipid layer permeation influx resistance for respiratory uptake	d $kg^{-\kappa}$	0.21	Hendriks and Heikens (2001)
$\rho_{lip,out}$	Lipid layer permeation efflux resistance	d $kg^{-\kappa}$	0.30	Hendriks and Heikens (2001)
κ_p^{II}	Lipid resistance exponents for inorganic mercury	dimensionless	0.57	Calibration procedure
κ_p^{MM}	Lipid resistance exponents for methyl-mercury	dimensionless	0.57	Calibration procedure
γ_0	Water absorption-excretion coefficient	kg^{κ} d^{-1}	200	Hendriks et al. (2001)
γ_1	Food ingestion coefficient	kg^{κ} d^{-1}	0.005	Hendriks et al. (2001)
γ_2	Biomass reproduction coefficient	kg^{κ} d^{-1}	0.0006	Hendriks et al. (2001)
K_{tw}^{II}	Dry tissue-water partition ratios for inorganic mercury	l kg^{-1}	5500	Calibration procedure
K_{tw}^{MM}	Dry tissue-water partition ratios for methyl-mercury	l kg^{-1}	11,000	Calibration procedure
$p_{s,phy}$	Dry fraction of phytoplankton	dimensionless	0.0768	Hendriks and Heikens (2001)
$p_{s,biv}$	Dry fraction of bivalvia	dimensionless	0.1698	Hendriks and Heikens (2001)
$p_{s,amp}$	Dry fraction of amphipoda	dimensionless	0.1652	Hendriks and Heikens (2001)
$p_{s,mys}$	Dry fraction of mysidacea	dimensionless	0.1517	Hendriks and Heikens (2001)
$p_{s,dec}$	Dry fraction of decapoda	dimensionless	0.1714	Hendriks and Heikens (2001)
$p_{s,pol}$	Dry fraction of polycheata	dimensionless	0.1715	Hendriks and Heikens (2001)
$p_{s,ost}$	Dry fraction of osteichthyes	dimensionless	0.1788	Hendriks and Heikens (2001)
q_T	Temperature correction factor for cold-blooded animal	dimensionless	1	Hendriks et al. (2001)
$p_{ass\_biv,Hg}^{II}$	Efficiency for dietary assimilation of inorganic mercury by bivalvia	dimensionless	0.03	Hendriks and Heikens (2001)
$p_{ass\_amp,Hg}^{II}$	Efficiency for dietary assimilation of inorganic mercury by amphipoda	dimensionless	0.16	Hendriks and Heikens (2001)
$p_{ass\_mys,Hg}^{II}$	Efficiency for dietary assimilation of inorganic mercury by mysidacea	dimensionless	0.16	Hendriks and Heikens (2001)
$p_{ass\_dec,Hg}^{II}$	Efficiency for dietary assimilation of inorganic mercury by decapoda	dimensionless	0.16	Hendriks and Heikens (2001)
$p_{ass\_pol,Hg}^{II}$	Efficiency for dietary assimilation of inorganic mercury by polychaeta	dimensionless	0.01	Calibration procedure
$p_{ass\_ost,Hg}^{II}$	Efficiency for dietary assimilation of inorganic mercury by osteichthyes	dimensionless	0.01	Hendriks and Heikens (2001)
$p_{ass\_fish,Hg}^{II}$	Efficiency for dietary assimilation of inorganic mercury by *M. barbatus*	dimensionless	0.01	Hendriks and Heikens (2001)
$p_{ass\_biv,MeHg}$	Efficiency for dietary assimilation of methyl-mercury by bivalvia	dimensionless	0.65	Hendriks and Heikens (2001)
$p_{ass\_amp,MeHg}$	Efficiency for dietary assimilation of methylmercury by amphipoda	dimensionless	0.60	Hendriks and Heikens (2001)
$p_{ass\_mys,MeHg}$	Efficiency for dietary assimilation of methyl-mercury by mysidacea	dimensionless	0.60	Hendriks and Heikens (2001)
$p_{ass\_dec,MeHg}$	Efficiency for dietary assimilation of methyl-mercury by decapoda	dimensionless	0.60	Hendriks and Heikens (2001)
$p_{ass\_pol,MeHg}$	Efficiency for dietary assimilation of methyl-mercury by polychaeta	dimensionless	0.99	Calibration procedure
$p_{ass\_ost,MeHg}$	Efficiency for dietary assimilation of methyl-mercury by osteichthyes	dimensionless	0.88	Hendriks and Heikens (2001)
$p_{ass\_fish,MeHg}$	Efficiency for dietary assimilation of methyl-mercury by *M. barbatus*	dimensionless	0.88	Hendriks and Heikens (2001)
$p'_{ass,biv}$	Fraction of ingested food assimilated by bivalvia	dimensionless	0.4	Hendriks et al. (2001)
$p'_{ass,amp}$	Fraction of ingested food assimilated by amphipoda	dimensionless	0.2	Hendriks et al. (2001)
$p'_{ass,mys}$	Fraction of ingested food assimilated by mysidacea	dimensionless	0.4	Hendriks et al. (2001)
$p'_{ass,dec}$	Fraction of ingested food assimilated by decapoda	dimensionless	0.8	Hendriks et al. (2001)
$p'_{ass,pol}$	Fraction of ingested food assimilated by polychaeta	dimensionless	0.2	Hendriks et al. (2001)
$p'_{ass,ost}$	Fraction of ingested food assimilated by osteichthyes	dimensionless	0.8	Hendriks et al. (2001)
$p'_{ass,fish}$	Fraction of ingested food assimilated by *M. barbatus*	dimensionless	0.8	Hendriks et al. (2001)
a	Initial growth coefficient	dimensionless	0.009	Calibration procedure
b	Allometric constant	dimensionless	3.07	Calibration procedure
L_∞	Asymptotic length of *M. barbatus*	mm	235	Tursi et al. (1996)
K	Growth coefficient of *M. barbatus*	y^{-1}	0.275	Tursi et al. (1996)
t'_0	Theoretical age of *M. barbatus* for length fixed to zero	y	−1.91	Tursi et al. (1996)

while they are weakly affected by mercury form dissolved in seawater.

The dynamics of Hg_i^{II} and $MeHg_i$ is modelled considering five biological processes:

i) mercury absorption through the invertebrate respiratory system (uptake term);
ii) absorption of the mercury incorporated in food and detritus through the invertebrate gastro-intestinal tract (GIT) (ingestion terms);
iii) mercury excretion through the invertebrate respiratory system (excretion term);
iv) excretion of mercury incorporated in food and detritus through the invertebrate GIT (egestion term);
v) excretion of mercury by dilution through the size growth of invertebrate (growth term).

In the Invertebrate Model, as well as for the Phytoplankton model, mercury absorption process for respiration is described by an uptake term with a first-order kinetics.

The mercury assimilation process in the GIT is reproduced for each invertebrate population through different ingestion terms, with a first-order kinetics, i.e. one term for each preferred diet component.

In particular, the ingestion term of the *i-th* invertebrate for the *j-th* prey is directly proportional to:

(i) the *dietary preference* of the *i-th* invertebrate for the *j-th* prey,
(ii) the *assimilation rate constant* of the *i-th* invertebrate,
(iii) the mercury content of the *j-th* prey.

The diet preferences of the invertebrates are considered constant, following the experimental findings reported in Catalano et al. (2014), Pipitone and Arculeo (2003) and Fauchald and Jumars (1979). The Hg excretion processes in the invertebrate are described by the egestion and growth terms, which are regulated by first-order kinetics. The egestion

rates are constant for both Hg^{II} and MeHg and are defined directly proportional to the *average invertebrate weight* with exponent -κ, and inversely proportional to the *dry fraction of invertebrate*, the *dry tissue-water partition ratio* for the MeHg and Hg^{II}, respectively, and the sum of:

(i) *water layer diffusion resistance experienced during exchange with invertebrate food,*
(ii) *lipid layer permeation efflux resistance corrected by temperature factor,*
(iii) *digestion flow delay.*

Thus, the kinetic model for the mercury concentrations in *i-th* invertebrate population is defined by the following ordinary differential equations:

$$\frac{dHg_i^{II}}{dt'} = k_{i,up\_ino}\cdot\left[Hg^{II}\right]_{z=z_b} + k_{i,ing\_ino}\cdot\left(Pref_{i,phy}\cdot Hg_{phy}^{II} + \sum_{j=1}^{6} Pref_{i,j}\cdot Hg_j^{II} + Pref_{i,SPM}\cdot Hg_{SPM}^{II} + Pref_{i,sed}\cdot Hg_{sed}^{II}\right) - Hg_i^{II}\cdot\left(k_{i,exc\_ino} + k_{i,ege\_ino} + k_{i,gr}\right) \tag{6}$$

where

- Hg_i^{II} and $MeHg_i$ are the IHg and MeHg concentrations in *i-th* invertebrate population, respectively $[\mu g\cdot kg_{wet\_wt}^{-1}]$;
- $k_{i,\ up\_uno}$ and $k_{i,\ up\_met}$ are the respiratory uptake rate constants of *i-th* invertebrate population for IHg and MeHg, respectively $[l\cdot kg_{wet\_wt}^{-1}\cdot d^{-1}]$;
- $[Hg^{II}]_{z=z_b}$ and $[MeHg]_{z=z_b}$ are the concentrations of IHg and MeHg in the deepest layer of seawater ($z = z_b$), respectively $[\mu g\cdot l^{-1}]$;
- $k_{i,\ ing\_ino}$ and $k_{i,\ ing\_met}$ are the assimilation rate constants of *i-th* invertebrate population for IHg and MeHg, respectively $[d^{-1}]$;
- $Pref_{i,\ phy}$, $Pref_{i,\ SPM}$ and $Pref_{i,\ sed}$ are the diet preferences of *i-th* invertebrate population for phytoplankton, SPM and sediments [*dimensionless*];
- $Pref_{i,\ j}$ are the diet preferences of *i-th* invertebrate population for *j-th* prey [*dimensionless*];
- Hg_{phy}^{II}, Hg_{sj}^{II}, Hg_{SPM}^{II} and Hg_{sed}^{II} are the IHg concentrations in phytoplankton, *j-th* prey, SPM and sediments, respectively $[\mu g\cdot kg_{wet\_wt}^{-1}]$;
- $MeHg_{phy}$, $MeHg_j$, $MeHg_{SPM}$ and $MeHg_{sed}$ are the MeHg concentrations in phytoplankton, *j-th* prey, SPM and sediments, respectively $[\mu g\cdot kg_{wet\_wt}^{-1}]$;
- $k_{i,\ exc\_ino}$ and $k_{i,\ exc\_met}$ are the excretion rate constants of *i-th* invertebrate population for IHg and MeHg, respectively $[d^{-1}]$;
- $k_{i,\ ege\_ino}$ and $k_{i,\ ege\_met}$ are the egestion rate constants of *i-th* invertebrate population for IHg and MeHg, respectively $[d^{-1}]$;
- $k_{i,\ gr}$ is *the* dilution rate constant associated with the size growth of *i-th* invertebrate population $[d^{-1}]$.

The rate constants of the Invertebrate Model are given by the following equations (following Hendriks and Heikens, 2001):

$$k_{i,up\_ino} = \frac{W_i^{-\kappa}}{\rho_w + \rho_{lip,in}\cdot[Hg^{II}]^{\kappa_p^{II}} + \frac{1}{\gamma_0}};\ k_{w,met,up} = \frac{W_i^{-\kappa}}{\rho_w + \rho_{lip,in}\cdot[MeHg]^{\kappa_p^{MM}} + \frac{1}{\gamma_0}} \tag{8}$$

$$k_{i,ing\_ino} = p_{ass\_i,Hg^{II}}\cdot q_T\cdot\gamma_1\cdot W_i^{-\kappa};\ k_{i,ing\_met} = p_{ass\_i,MeHg}\cdot q_T\cdot\gamma_1\cdot W_i^{-\kappa} \tag{9}$$

$$k_{i,exc\_ino} = \frac{1}{K_{tw}^{II}\cdot p_{s,i}}\cdot\frac{W_i^{-\kappa}}{\rho_w + \rho_{lip,out} + \frac{1}{\gamma_0}};\ k_{i,exc\_ino} = \frac{1}{K_{tw}^{MM}\cdot p_{s,i}}\cdot\frac{W_i^{-\kappa}}{\rho_w + \rho_{lip,out} + \frac{1}{\gamma_0}} \tag{10}$$

$$k_{i,ege\_ino} = \frac{1}{K_{tw}^{II}\cdot p_{s,i}}\cdot\frac{W_i^{-\kappa}}{\rho_{w,ege} + \frac{\rho_{lip,out}}{q_T} + \frac{1}{p_{s,food\_i}\cdot K_{tw}^{II}\cdot\left(1-p'_{ass,i}\right)\cdot q_T\cdot\gamma_1}}; \tag{11}$$

$$k_{i,ege\_met} = \frac{1}{K_{tw}^{MM}\cdot p_{s,i}}\cdot\frac{W_i^{-\kappa}}{\rho_{w,ege} + \frac{\rho_{lip,out}}{q_T} + \frac{1}{p_{s,food\_i}\cdot K_{tw}^{MM}\cdot\left(1-p'_{ass,i}\right)\cdot q_T\cdot\gamma_1}};\quad k_{i,gr} = q_T\cdot\gamma_2\cdot W_i^{-\kappa} \tag{12}$$

where

- W_i is *the* average weight of *i-th* invertebrate $[kg_{wet\_w}]$;
- κ is the rate exponent [dimensionless];
- ρ_w is the water layer diffusion resistance $[d\cdot kg^{-\kappa}]$;
- $\rho_{lip,\ in}$ is the lipid *layer* permeation influx resistance $[d\cdot kg^{-\kappa}\cdot\mu g^{-\kappa_p}\cdot l^{\kappa_p}]$;
- κ_p^{II} and κ_p^{MM} are the lipid layer resistance exponents for IHg and MeHg, respectively [dimensionless];

$$\frac{dMeHg_i}{dt'} = k_{i,up\_met}\cdot[MeHg]_{z=z_b} + k_{i,ing\_met}\cdot\left(Pref_{i,phy}\cdot MeHg_{phy} + \sum_{j=1}^{6} Pref_{i,j}\cdot MeHg_j + Pref_{i,SPM}\cdot MeHg_{SPM} + Pref_{i,sed}\cdot MeHg_{sed}\right) - MeHg_i\cdot\left(k_{i,exc\_met} + k_{i,ege\_met} + k_{i,gr}\right) \tag{7}$$

- γ_0 is the water *absorption*-excretion coefficient $[kg^{\kappa}\cdot d^{-1}]$;
- $p_{ass\_i,\ Hg^{II}}$ and $p_{ass\_i,\ MeHg}$ are, respectively, the efficiencies for dietary assimilation of IHg and MeHg by *i-th* invertebrate population [dimensionless];
- q_T is the temperature correction factor [dimensionless];
- γ_1 is the food *ingestion* coefficient $[kg^{\kappa}\cdot d^{-1}]$;
- K_{tw}^{II} and K_{tw}^{MM} are the dry tissue-water partition ratios for IHg and MeHg, respectively $[kg_{dry\_wt}^{-1}/l^{-1}]$;
- $p_{s,\ i}$ is the dry *fraction* of *i-th* invertebrate population $[kg_{dry\_wt}/kg_{wet\_wt}]$;
- $\rho_{lip,\ out}$ is the lipid *layer* permeation efflux resistance $[d\cdot kg^{-\kappa}]$;
- $\rho_{w,\ ege}$ is the water *layer* diffusion resistance for assimilation of chemicals from food $[d\cdot kg^{-\kappa}]$;
- $p_{s,\ food\_i}$ is the dry *fraction* of food for *i-th* invertebrate $[kg_{dry\_wt}/kg_{wet\_wt}]$;
- $p'_{ass,\ i}$ is the fraction of ingested food assimilated by *i-th* invertebrate [dimensionless];
- γ_2 is the biomass *reproduction* coefficient $[kg^{\kappa}\cdot d^{-1}]$.

Table 1 reports the model parameters which, except for W_i and $p_{s,\ food\_i}$, are fixed following the empirical results obtained by Hendriks and Heikens (2001) and Hendriks et al. (2001). The average weights of invertebrate populations are set according to the available literature (Campfens and Mackay, 1997; McKinney et al., 2004; Radomyski and Ciffroy, 2015b; Yakovlev and Yakovleva, 2010). The dry fraction of the food of each invertebrate is calculated as follows:

$$p_{s,food\_i} = \sum_{j=1}^{n} Pref_{i,j}\cdot p_{s,j} \tag{13}$$

where $p_{s,\ j} = 0.20\cdot W_j^{0.03}$.

The *lipid resistance exponents* (κ_p^{II} and κ_p^{MM}) and the *dry tissue-water partition ratios* (K_{tw}^{II} and K_{tw}^{MM}) are the same used in the Phytoplankton Model and are calibrated in order to better reproduce the mercury concentrations observed in marine organisms (Section 3).

2.4. Fish model

The dynamics of mercury concentration in fish has been analyzed using the Fish Model, specialized to the red mullet target species (*M. barbatus*). The direct interactions with seawater and invertebrates supporting the diet preferences of fish are modelled respectively by the uptake term and ingestion terms of the ODEs of the Fish Model. On the other hand, the indirect interactions with the other components of marine environment (SPM, sediment, phytoplankton, other aquatic organisms etc.) are calculated using the ODEs for both the Phytoplankton Model (Paragraph 2.2) and the Invertebrate Model (Paragraph 2.3).

In general, the Hg content in fish primarily depends on the concentrations of the metal in ingested invertebrates (polychaeta, decapoda, bivalvia, etc.), derived by the Invertebrate Model, while they are very weakly affected by mercury concentrations in seawater, as estimated by the HR3DHG Model (Denaro et al., 2020).

The diet preferences are obtained by using the experimental findings reported by Esposito et al. (2014) and based on the fish food web, from phytoplankton to invertebrates, taking into account the information available on prey living in the Augusta Bay (Catalano et al., 2014). An illustration of the diet preferences (depending on the depth, age and availability of prey present in the benthic community) used in the INTFISH model is reported in Fig. 2.

Eqs. (14)–(24) describe the model for reproducing the dynamics of both Hg^{II} and MeHg in fish in the considered area. Specifically, we reproduced the behaviour of the both mercury species in a fish placed in the position (x,y) of seabed at a specific age (t'), i.e. $Hg^{II}_{fish}(x,y,t')$ and $MeHg^{II}_{fish}(x,y,t')$. Moreover, the model allows us to calculate both the Hg^{TOT} concentration (Hg^{TOT}_{fish}) by adding the concentrations of the two mercury species, as well as the ratio between the MeHg concentration and the Hg^{TOT} concentration inside the fish body.

The dynamics of mercury is not affected by the initial conditions of the Fish Model. Moreover, the Hg^{TOT} concentration calculated at fish capture is not affected significantly by the dynamics of mercury concentrations during the first year of life.

The dynamics of Hg^{II} and MeHg are modelled by considering five biological processes already considered in the Invertebrate Model. In particular, all mercury uptake and elimination processes are described by terms with a first-order kinetics.

The ingestion term of the fish for the *j-th* prey is directly proportional to

(i) the fish *diet preference* for the *j-th* prey,
(ii) the *assimilation rate constant*,
(iii) the mercury content of the *j-th* prey.

In particular, the *diet preferences* are fixed as constant functions for the whole juvenile stage (t' < 2 years), when *M. barbatus'* diet is similar to that of other demersal fish. During the transition from the juvenile stage to the full maturity stage ($2 \leq t' < 3$ years), the *diet preferences* change as a function of time, due to the progressive loss of premaxillary teeth (Esposito et al., 2014). Finally, the *diet preferences* are fixed as constant after the achievement of full maturity stage (t' ≥ 3 years), when the *M. barbatus* definitively assumes the feeding pattern typical of a benthic fish.

All these parameters, except for the *dry fraction* and the fish *weight*, are fixed as constant for the whole fish lifetime according to previous works (Hendriks et al., 2001; Hendriks and Heikens, 2001). Differently, the fish *dry fraction* depends on its weight, and therefore it changes as a function of time.

The fish growth rate constant changes as a function of time, and is defined as a function of the *temperature correction factor*, the *biomass production coefficient* and the *weight* with exponent -κ.

Overall, the kinetic model for the mercury concentrations in fish is given by the following ODEs (Hendriks et al., 2001; Hendriks and Heikens, 2001; Radomyski and Ciffroy, 2015c):

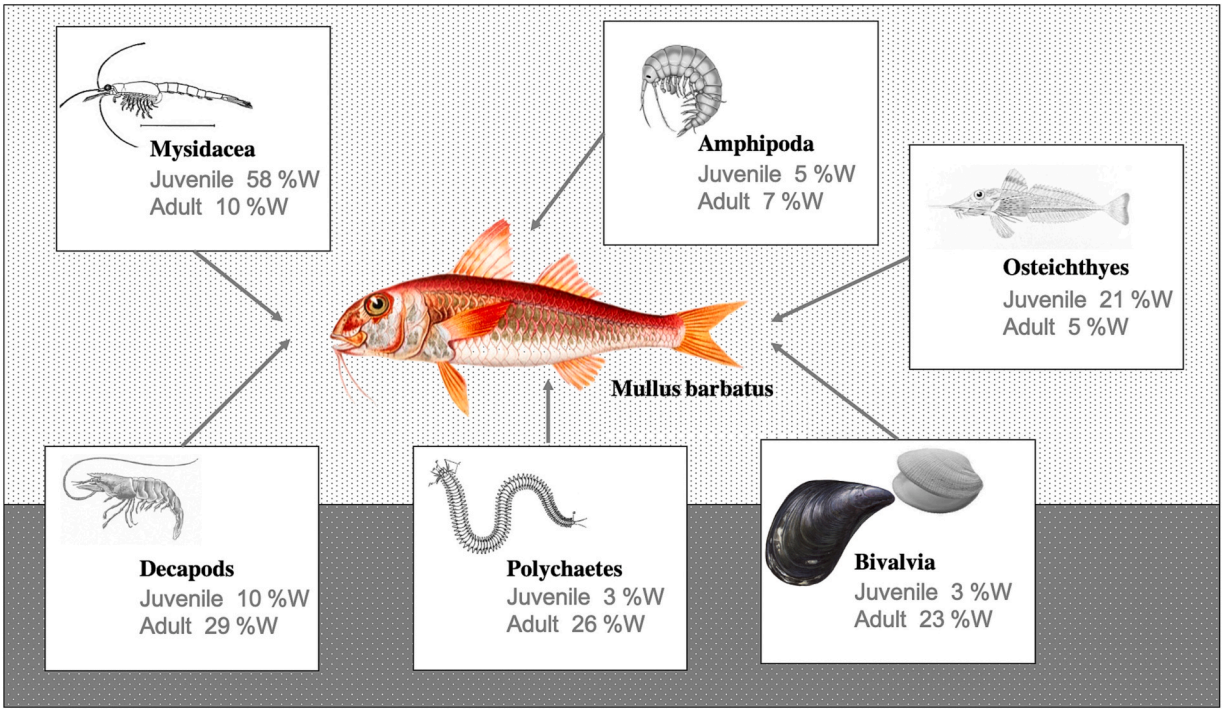

Fig. 2. Graphical representation of diet composition of *M. barbatus* with percentage of preference (percentage by weight -%W) in the two different age stage (juvenile and adult). The diet preferences are obtained by using the experimental findings reported in Esposito et al., 2014 and the information on prey from Catalano et al., 2014.

$$\begin{cases}
\frac{dHg^{II}_{fish}}{dt'} = k_{fish,up_ino}(t')\cdot\left[Hg^{II}(x_r,y_r,t')\right]_{z=z_b} + k_{fish,ing_ino}(t')\cdot\sum_{j=1}^{6} Pref_{jun_fish,j}\cdot Hg^{II}_{j}(x_r,y_r,t') \\
\quad -Hg^{II}_{fish}\cdot\left(k_{fish,exc_{ino}}(t') + k_{fish,ege_{ino}}(t') + k_{fish,gr}(t')\right) for\ 0 < t' \le 1\ year \\
\frac{dHg^{II}_{fish}}{dt'} = k_{fish,up_ino}(t')\cdot\left[Hg^{II}(x_f,y_f,t')\right]_{z=z_b} + k_{fish,ing_ino}(t')\cdot\sum_{j=1}^{6} Pref_{juv_fish,j}\cdot Hg^{II}_{j}(x_f,y_f,t') \\
\quad -Hg^{II}_{fish}\cdot\left(k_{fish,exc_{ino}}(t') + k_{fish,ege_{ino}}(t') + k_{fish,gr}(t')\right) for\ 1 < t' \le 2\ years \\
\frac{dHg^{II}_{fish}}{dt'} = k_{fish,up_ino}(t')\cdot\left[Hg^{II}(x_f,y_f,t')\right]_{z=z_b} + k_{fish,ing_ino}(t')\cdot\sum_{j=1}^{6} Pref_{fish,j}(t')\cdot Hg^{II}_{j}(x_f,y_f,t') \\
\quad -Hg^{II}_{fish}\cdot\left(k_{fish,exc_{ino}}(t') + k_{fish,ege_{ino}}(t') + k_{fish,gr}(t')\right) for\ 2 < t' \le 3\ years \\
\frac{dHg^{II}_{fish}}{dt'} = k_{fish,up_ino}(t')\cdot\left[Hg^{II}(x_f,y_f,t')\right]_{z=z_b} + k_{fish,ing_ino}(t')\cdot\sum_{j=1}^{6} Pref_{mat_fish,j}\cdot Hg^{II}_{j}(x_f,y_f,t') \\
\quad -Hg^{II}_{fish}\cdot\left(k_{fish,exc_{ino}}(t') + k_{fish,ege_{ino}}(t') + k_{fish,gr}(t')\right) for\ 3\ years < t' \le AGE_{death}
\end{cases} \tag{14}$$

$$\begin{cases}
\frac{dMeHg_{fish}}{dt'} = k_{fish,up_{met}}(t')\cdot[MeHg(x_r,y_r,t')]_{z=z_b} \\
\quad +k_{fish,ing_met}(t')\cdot\sum_{j=1}^{6} Pref_{jun_fish,j}\cdot MeHg_j(x_r,y_r,t') \\
\quad -MeHg_{fish}\cdot\left(k_{fish,exc_{met}}(t') + k_{fish,ege_{met}}(t') + k_{fish,gr}(t')\right) for\ 0 < t' \le 1\ year \\
\frac{dMeHg_{fish}}{dt'} = k_{fish,up_{met}}(t')\cdot\left[MeHg(x_f,y_f,t')\right]_{z=z_b} \\
\quad +k_{fish,ing_met}(t')\cdot\sum_{j=1}^{6} Pref_{juv_fish,j}\cdot MeHg_j(x_f,y_f,t') \\
\quad -MeHg_{fish}\cdot\left(k_{fish,exc_{met}}(t') + k_{fish,ege_{met}}(t') + k_{fish,gr}(t')\right) for\ 1 < t' \le 2\ years \\
\frac{dMeHg_{fish}}{dt'} = k_{fish,up_{met}}(t')\cdot\left[MeHg(x_f,y_f,t')\right]_{z=z_b} \\
\quad +k_{fish,ing_met}(t')\cdot\sum_{j=1}^{6} Pref_{fish,j}(t')\cdot MeHg_j(x_f,y_f,t') \\
\quad -MeHg_{fish}\cdot\left(k_{fish,exc_{met}}(t') + k_{fish,ege_{met}}(t') + k_{fish,gr}(t')\right) for\ 2 < t' \le 3\ years \\
\frac{dMeHg_{fish}}{dt'} = k_{fish,up_{met}}(t')\cdot\left[MeHg(x_f,y_f,t')\right]_{z=z_b} \\
\quad +k_{fish,ing_met}(t')\cdot\sum_{j=1}^{6} Pref_{mat_fish,j}\cdot MeHg_j(x_f,y_f,t') \\
-MeHg_{fish}\cdot\left(k_{fish,exc_{met}}(t') + k_{fish,ege_{met}}(t') + k_{fish,gr}(t')\right) for\ 3\ years < t' \le AGE_{death}
\end{cases} \tag{15}$$

where

- Hg^{II}_{fish} and $MeHg_{fish}$ are the Hg^{II} and MeHg concentrations in fish, respectively [$\mu g \cdot kg^{-1}_{wet\_wt}$];
- $k_{fish,\ up\_ino}(t')$ and $k_{fish,\ up\_met}(t')$ are the respiratory uptake rate constants for Hg^{II} and MeHg, respectively [$l \cdot kg^{-1}_{wet\_wt} \cdot d^{-1}$];
- $[Hg^{II}(x_r,y_r,t')]_{z=z_b}$ and $[MeHg(x_r,y_r,t')]_{z=z_b}$ are the Hg^{II} and MeHg concentrations at the seabed ($z = z_b$) of the mouth of the river (x_r, y_r), respectively [$\mu g\, l^{-1}$];
- $[Hg^{II}(x_f,y_f,t')]_{z=z_b}$ and $[MeHg(x_f,y_f,t')]_{z=z_b}$ are the Hg^{II} and MeHg concentrations at the seabed ($z = z_b$) of point (x_f, y_f) where the fish is caught, respectively [$\mu g\, l^{-1}$];
- $k_{fish,\ ing\_ino}(t')$ and $k_{fish,\ ing\_met}(t')$ are the fish assimilation rate constants for Hg^{II} and MeHg, respectively [d^{-1}];
- $Pref_{juv\_fish,\ j}$ are the diet preferences at the juvenile stage for the *j-th* prey [dimensionless];

- $Pref_{fish,\ j}(t')$ are the diet preferences for the *j-th* prey during the transition from the juvenile stage to the full maturity stage [dimensionless];
- $Pref_{mat\_fish,\ j}$ are the diet preferences at full maturity stage for the *j-th* prey [dimensionless];
- Hg_j^{II} and $MeHg_j$ are the Hg^{II} and MeHg concentrations in the *j-th* prey, respectively $[\mu g \cdot kg_{wet\_wt}^{-1}]$;
- $k_{fish,\ exc\_ino}(t')$ and $k_{fish,\ exc\_met}(t')$ are the excretion rate constants for Hg^{II} and MeHg, respectively $[d^{-1}]$;
- $k_{fish,\ ege\_ino}(t')$ and $k_{fish,\ ege\_met}(t')$ are the egestion rate constants for Hg^{II} and MeHg, respectively $[d^{-1}]$;
- $k_{fish,\ gr}(t')$ is *the* growth rate constant associated with the progressive fish size increase $[d^{-1}]$;
- $AGE_{capture}$ is the fish age at capture [y].

All rate constants of the Fish Model are calculated assuming a behaviour of MeHg similar to that of inorganic compounds (Hendriks and Heikens, 2001). Accordingly, the rate constants of the Fish Model are defined by following equations:

$$k_{fish,up\_ino}(t') = \frac{W_{fish}^{-\kappa}(t')}{\rho_w + \rho_{lip,in}\cdot[Hg^{II}(x_r,y_r,t')]^{\kappa_p^{II}} + \frac{1}{\gamma_0}};$$
$$k_{fish,up\_met}(t') = \frac{W_{fish}^{-\kappa}(t')}{\rho_w + \rho_{lip,in}\cdot[MeHg(x_r,y_r,t')]^{\kappa_p^{MM}} + \frac{1}{\gamma_0}}\ for\ 0 < t' \le 1\ y. \tag{16}$$

$$k_{fish,up\_ino}(t') = \frac{W_{fish}^{-\kappa}(t')}{\rho_w+\rho_{lip,in}\cdot[Hg^{II}(x_f,y_f,t')]^{\kappa_p^{II}}+\frac{1}{\gamma_0}};$$
$$k_{fish,up\_met}(t') = \frac{W_{fish}^{-\kappa}(t')}{\rho_w+\rho_{lip,in}\cdot[MeHg(x_f,y_f,t')]^{\kappa_p^{MM}}+\frac{1}{\gamma_0}}\ for\ 1\ y < t' \le AGE_{death}$$

$$k_{fish,ing_{ino}}(t') = p_{ass_{fish},Hg^{II}}\cdot q_T\cdot\gamma_1\cdot W_{fish}^{-\kappa}(t'); k_{fish,ing\_met}(t')$$
$$= p_{ass\_fish,MeHg}\cdot q_T\gamma_1 W_{fish}^{-\kappa}(t') \tag{17}$$

$$k_{fish,exc\_ino}(t') = \frac{1}{K_{tw}^{II}\cdot p_{s,fish}(t')}\cdot\frac{W_{fish}^{-\kappa}(t')}{\rho_w + \rho_{lip,out} + \frac{1}{\gamma_0}}; k_{fish,exc\_met}(t')$$
$$= \frac{1}{K_{tw}^{MM}\cdot p_{s,fish}(t')}\cdot\frac{W_{fish}^{-\kappa}(t')}{\rho_w + \rho_{lip,out} + \frac{1}{\gamma_0}} \tag{18}$$

$$k_{fish,ege\_ino}(t') = \frac{1}{K_{tw}^{II}\cdot p_{s,fish}(t')}\cdot\frac{W_{fish}^{-\kappa}(t')}{\rho_{w,ege} + \frac{\rho_{lip,out}}{q_T} + \frac{1}{p_{s,food\_fish}(t')\cdot K_{tw}^{II}\cdot(1-p'_{ass,fish})\cdot q_T\cdot\gamma_1}}; \tag{19}$$

$$k_{fish,ege\_met}(t') = \frac{1}{K_{tw}^{MM}\cdot p_{s,fish}(t')}\cdot\frac{W_{fish}^{-\kappa}(t')}{\rho_{w,ege} + \frac{\rho_{lip,out}}{q_T} + \frac{1}{p_{s,food\_fish}(t')\cdot K_{tw}^{MM}\cdot(1-p'_{ass,fish})\cdot q_T\cdot\gamma_1}}$$

$$k_{fish,gr}(t') = q_T\cdot\gamma_2\cdot W_{fish}^{-\kappa}(t') \tag{20}$$

where

- $W_{fish}(t')$ is the fish weight at age t' $[kg_{wet\_w}]$;
- κ is the rate exponent [dimensionless];
- ρ_w is the water layer diffusion resistance $[d\cdot kg^{-\kappa}]$;
- $\rho_{lip,\ in}$ is *the* lipid layer permeation influx resistance $[d\cdot kg^{-\kappa}\cdot\mu g^{-\kappa_p}\cdot l^{\kappa_p}]$;
- κ_p^{II} and κ_p^{MM} are the lipid layer resistance exponents for Hg^{II} and MeHg, respectively [dimensionless];
- γ_0 is the water absorption-excretion coefficient $[kg^{\kappa}\cdot d^{-1}]$;
- $p_{ass\ fish,\ Hg^{II}}$ and $p_{ass\ fish,\ MeHg}$ are the efficiencies for dietary assimilation of Hg^{II} and MeHg, respectively [dimensionless];
- q_T is the temperature correction factor [dimensionless];
- γ_1 is the food ingestion coefficient $[kg^{\kappa}\cdot d^{-1}]$;
- K_{tw}^{II} and K_{tw}^{MM} are the dry tissue-water partition ratios for Hg^{II} and MeHg, respectively $[kg_{dry\_wt}^{-1}/l^{-1}]$;
- $p_{s,\ fish}(t')$ is the dry fraction of fish at age t' $[kg_{dry\_wt}/kg_{wet\_wt}]$;
- $\rho_{lip,\ out}$ is the lipid layer permeation efflux resistance $[d\cdot kg^{-\kappa}]$;
- $\rho_{w,\ ege}$ is the water layer diffusion resistance for assimilation of chemicals from food $[d\cdot kg^{-\kappa}]$;
- $p_{s,\ food\ fish}(t')$ is the dry fraction of the food at age t' $[kg_{dry\_wt}/kg_{wet\_wt}]$;
- $p'_{ass,\ fish}$ is the fraction of ingested food assimilated [dimensionless];
- γ_2 is the biomass reproduction coefficient $[kg^{\kappa}\cdot d^{-1}]$.

Table 1 reports the Fish model parameters which, except for $W_{fish}(t')$, $p_{s,fish}(t')$, and $p_{s,food\text{-}fish}(t')$, are set using information from the available literature (Hendriks et al., 2001; Hendriks and Heikens, 2001).

The temporal behaviour of fish weight is reproduced by using the following Richards equation (Alia, 2015; Bianchini and Ragonese, 2011; Cadima, 2003):

$$W_{fish}(t') = a\cdot\left[L_{fish}\cdot(t')\right]^b \tag{21}$$

where *a* is the initial growth coefficient, *b* is the allometric constant and the fish length L_{fish} [mm] is evaluated by using the von Bertalanffy growth equation (Beverton and Holt, 1956; Von Bertalanffy, 1934; Von Bertalanffy, 1938; Von Bertalanffy, 1949; Von Bertalanffy, 1957):

$$L_{fish}(t') = L_{\infty}\cdot\left[1 - exp\left(-K\left(t' - t_0'\right)\right)\right] \tag{22}$$

where t_0' is the fish theoretical age for length fixed to zero [y], $L_{\infty}$is the asymptotic length of fish [mm], and*K* is the fish growth coefficient [1/y].

The parameters *a* and *b* are calibrated by using the fish lengths and weights caught in October 2017 (Alia, 2015), while the parameters L_{∞}, *K*and t_0' are fixed equal to those estimated by Tursi et al. (1996) for *M. barbatus* living in the Ionian Sea (Bianchini and Ragonese, 2011).

In order to compare the model outputs with experimental data, we calculate the HgTOT concentration in fish at the moment of capture: May 2012 (Bonsignore et al., 2013) and October 2017 (Di Bella et al., 2020). The age of each specimen of fish at capture ($AGE_{capture}$) was calculated by adopting the inverse function of the von Bertalanffy growth (Eq. (22)). In particular, for fixed parameters, we calculate the age at capture (t' = $AGE_{capture}$) by using the fish length ($L_{fish}(t') = L_{fish}(-AGE_{death})$) measured experimentally after it was caught. We fix the starting time of each simulation for the Phytoplankton, Invertebrate and Fish Models (t' = 0), to the birth date of each specimen (t = t_{birth}) in the temporal domain of the biogeochemical model.

The *dry fraction* of fish as a function of age is calculated by using the following empirical equation (Hendriks and Heikens, 2001):

$$p_{s,fish}(t') = 0.20\cdot W_{fish}^{0.03}(t') \tag{23}$$

The *dry fraction of the food* as a function of age is calculated as follows (Hendriks and Heikens, 2001):

$$\begin{cases} p_{s,food_{fish}}(t') = \sum_{j=1}^{n} Pref_{jun_{fish,j}}\cdot p_{s,j}\ for\ 0 < t' \le 2\ years \\ p_{s,food_{fish}}(t') = \sum_{j=1}^{n} Pref_{fish,j}(t')\cdot p_{s,j}\ for\ 2\ years < t' \le 3\ years \\ p_{s,food_{fish}}(t') = \sum_{j=1}^{n} Pref_{mat_{fish,j}}\cdot p_{s,j}\ for\ 3\ years < t' \le AGE_{death} \end{cases} \tag{24}$$

where

$$p_{s,j} = 0.20\cdot W_j^{0.03}\ \text{and}\ Pref_{fish,j}(t') = Pref_{jun\_fish,j} + \frac{Pref_{mat\_fish,j} - Pref_{jun\_fish,j}}{\Delta t_{tr}'}\cdot t' \tag{25}$$

Here, W_j is the average weight of the *j-th* invertebrate, and $\Delta t_{tr}'$ is the transition time from the juvenile stage to the full maturity stage (1 year).

The values of parameters of Eq. (25) are the same as those used in the Richards equation (Table 1).

The *lipid resistance exponents* (κ_p^{II} and κ_p^{MM}) and the *dry tissue-water partition ratios* (K_{tw}^{II} and K_{tw}^{MM}) are the same used both in Phytoplankton Model and Invertebrate Model and are calibrated in such a way to reproduce the Hg^{TOT} concentration observed in marine organisms of the Augusta Bay (see Section 3).

The Fish Model ODEs provide a different non-steady solution for each stage of the fish life cycle, since the spatial distributions of mercury concentrations in seawater, suspended particulate matter (SPM), sediments, phytoplankton and invertebrates are obtained at non-steady state (Denaro et al., 2020).

2.5. Model and simulation setup

INTFISH is coded in C++ and uses the forward Euler method for temporal discretization. Since the integrated models are coupled in real time with the HR3DHG Model, the same time step (300 s) has been fixed. Specifically, the time step was chosen to guarantee the convergence and stability conditions associated with the numerical methods adopted for the HR3DHG Model. The methods adopted for the spatial discretization of PDEs of HR3DHG model are reported by Denaro et al. (2020), where for the case study of Augusta Bay a 3D grid constituted by a mesh of 10×18 elements regularly spaced of 454.6 m in both x- and y-direction is adopted, with a variable number of vertical layers of 5 m depth in the z-direction. The simulation time (t') for the Fish Model starts at the recruitment time and finishes at the death of fish, namely at the moment of capture.

The Hg concentrations in all marine organisms (phytoplankton, invertebrates and fish) at simulation initial time ($t' = 0$), are obtained by setting to zero the time derivative of the ODEs of the integrated Fish model.

The HR3DHG Model results were obtained by running a single long simulation up to $t_{max} = 13$ years, corresponding to the second sampling period (October 2017). Simultaneously, we integrated the ODEs of the Fish Model from the birth date ($t' = 0$ and $t = t_{birth}$) to the capture date ($t' = AGE_{capture}$ and $t = t_{death}$) in order to reproduce the Hg^{TOT} concentration at the time of fish capture. The birth date ($t = t_{birth}$) was obtained by subtracting the age at death from the death date, while its death date ($t = t_{death}$) was fixed in agreement with the catching date.

Concerning the calibration procedure, as a first step we optimized the initial growth coefficient (a) and the allometric constant (b) of the Eq. (21) in such a way as to achieve the best fit between the theoretical results and experimental data for the weights of six specimens collected in October 2017. Then, we fixed the *dry tissue-water partition ratio* for MeHg in such a way as to obtain, in accordance with previous works (Storelli et al., 2003, 2005), the highest ratio between the MeHg concentration and Hg^{TOT} concentration in the muscle tissue of all the fish specimens, and to respect the value range empirically obtained by Hendriks and Heikens (2001) for the inorganic chemicals. According to this, we also calculated the *dry tissue-water partition ratio* for Hg^{II}, which has been set equal to a half of the *dry tissue-water partition ratio* for MeHg (Hendriks and Heikens, 2001). As a third step, we calibrated the *efficiencies for dietary assimilation* of Hg^{II} and MeHg by polychaeta, i.e. the only one invertebrate for which these parameters were unknown. Specifically, these assimilation efficiencies were optimized to obtain the highest ratio between the MeHg and Hg^{TOT} concentration in fish muscle, and to better reproduce the Hg^{TOT} concentration in polychaeta (Bizzotto et al., 2014; Catalano et al., 2014). As a fourth step, we calibrated the *lipid layer resistance exponents* for both Hg species to optimize the match between theoretical results and experimental data, and to better reproduce the empirical results obtained by Hendriks and Heikens (2001). To this end, the value of both exponents was initially fixed equal to 0.530 according to Hendriks and Heikens (2001). Afterwards, the *lipid layer resistance exponents* were optimized to obtain the best fit between the theoretical results and experimental data for Hg^{TOT} concentration measured in the muscle tissue of *M. barbatus* caught during the first sampling period (May 2012). The calibrated *lipid layer resistance exponents* ($\kappa_p^{II} = \kappa_p^{MM} = 0.57$) were in good agreement with empirical findings previously reported by Hendriks and Heikens (2001).

The dynamics of fish weight was reproduced by using the Richards equation (Alia, 2015; Bianchini and Ragonese, 2011; Cadima, 2003), whose parameters were fixed in such a way as to simulate the growth of red mullets populating the Augusta Bay (Bianchini and Ragonese, 2011; Tursi et al., 1996). We also calculated the fish *dry fraction* according to the empirical function by Hendriks and Heikens (2001). The dynamics of the food *dry fraction* was calculated as a function of the dry fractions of invertebrates and the fish diet preferences. The former was fixed for the whole lifetime of red mullet, while the latter changed as a function of age (Esposito et al., 2014).

The integrated Fish Model was coupled with the HR3DHG Model, run by considering seasonal variability (and including dynamics of water currents, wind etc.) and fed by hydrodynamic modelling inputs from the SHYFEM model (Cucco et al., 2016; Cucco et al., 2019; De Marchis et al., 2014; Massel, 1999; Umgiesser, 2009; Umgiesser et al., 2014).

3. Results and discussion

The Hg^{TOT} concentrations (as sum of Hg^{II} and MeHg) in fish were estimated solving the INTFISH eqs. (1)–(25) for specimens caught in Augusta Bay during both sampling periods (Fig. 3 and Table 3), (Bonsignore et al., 2013; Di Bella et al., 2020). The model also reproduces the spatial distribution of Hg^{TOT} in phytoplankton and invertebrates in the study area. Mercury concentrations in seawater and sediments were calculated, in non-steady conditions, by the HR3DHG Model (Denaro et al., 2020), which takes also into account the seasonal changes of environmental variables.

In comparison to recent related work in this field, our hierarchical mechanistic modelling approach is able to enhance the understanding of mercury bioaccumulation processes and its prediction capabilities, even in presence of scarce calibration data. This framework is similar to the ecophysiological prey-predator approach proposed by (Ni et al., 2017; Ni and Arhonditsis, 2023), but we here consider a higher variety of prey and more trophic levels; physiological modelling is substantially different from a purely Bayesian framework such as the one followed in (Mahmood et al., 2013), based on series of dynamic linear models (DLMs) to examine temporal trends of toxicants, or from the statistical multilevel modelling of (Visha et al., 2021), useful to deal with nested data, or from the learning method proposed by (Kobayashi and Yoshida, 2021), exploiting gradient boosting decision trees (GBDTs).

Moreover, the calibration procedure performed by using the experimental data allows to improve the estimation of additional parameters with respect to previous works:

- the dynamics of fish weight growth, reproduced throughout the whole fish life cycle using the Richards equation;
- the real diet preferences of each considered marine organism in the food web;
- the fish displacements within the considered area and the dietary changes during the different stages of life.

The average $MeHg/Hg^{TOT}$ ratio significantly increases along the food chain from phytoplankton to red mullet. In particular, most of the mercury in this species is in methylated form (84.4%) while 15.6% is in inorganic form. Conversely, the ratio is approximately reversed in phytoplankton (11.1% of MeHg and 88.9% of Hg^{II}) and in some crustacea, such as amphipoda, mysidacea and decapoda (Table 2).

The model confirms the presence of primary bioaccumulation processes, which involve the MeHg form and its transfer in the higher levels of marine food web. In particular, the numerical results well describe the increase of Hg^{TOT} along the food chain, from seawater (trophic level 0)

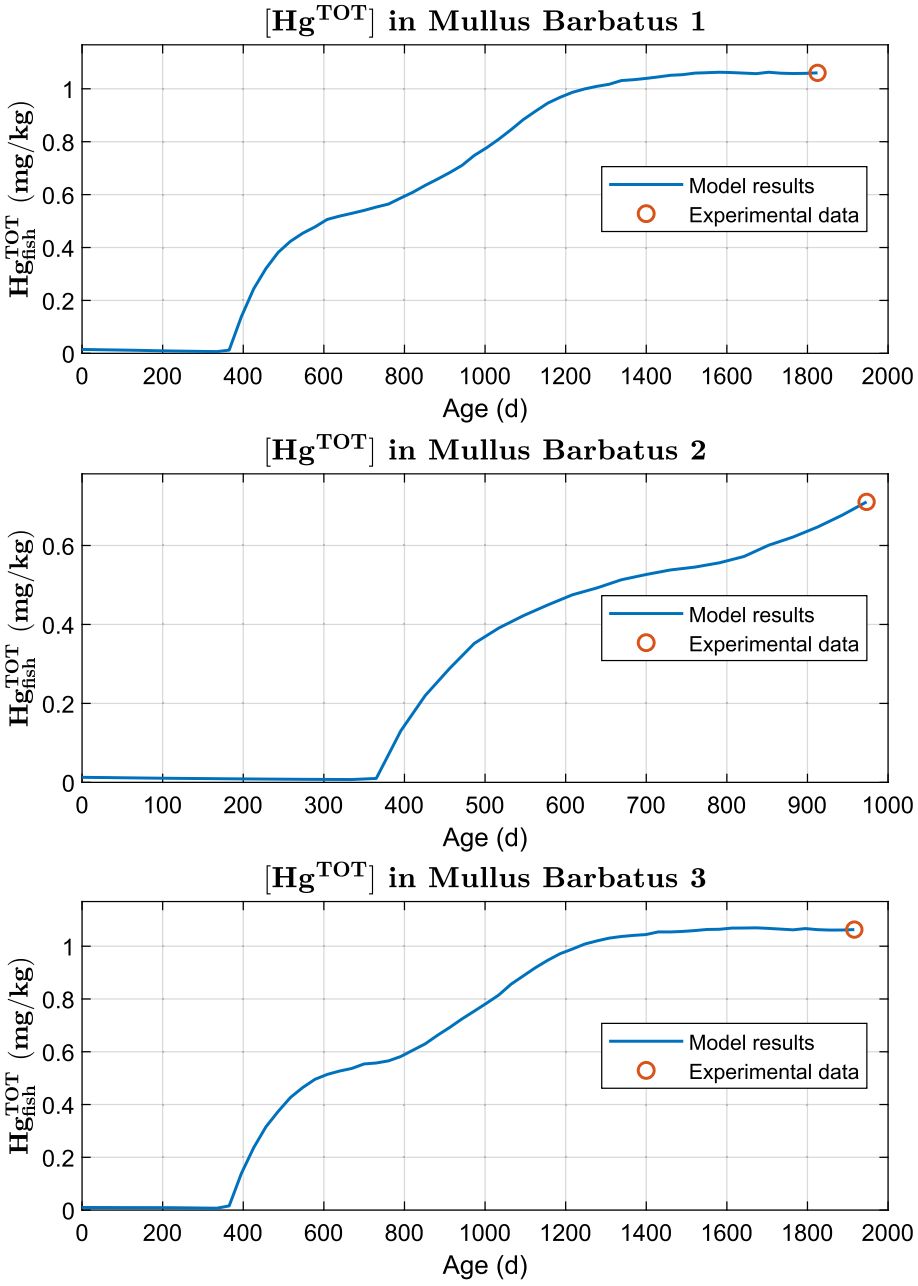

Fig. 3. Dynamics of the Hg^{TOT} concentration in three *M. barbatus* specimens caught in the Augusta Bay during the first sampling (May 2012). The blue lines show the Hg^{TOT} concentration as a function of age obtained by the Integrated Fish Model. The red circles represent the Hg^{TOT} concentrations measured in three caught samples. (For interpretation of the references to colour in this figure legend, the reader is referred to the web version of this article).

Table 2
Percentage of MeHg and HgII obtained by INTFISH for the marine organisms. The percentage values for *M. barbatus* are calculated for samples collected in May 2012 (Bonsignore et al., 2013).

Population	Trophic level	MeHg	Hg^{II}
		%	%
Phytoplankton	1	11.1	88.9
Amphipoda	2	13.8	86.2
Mysidacea	2	14.8	85.2
Decapoda	2	14.4	85.6
Bivalvia	2	17.4	82.6
Polychaeta	2	26.0	74.0
Osteichthyes	2.5	84.5	15.5
M. barbatus	3	84.4	15.6

to invertebrates (trophic level 2), as suggested in the literature (Leonard et al., 1995; Watras and Bloom, 1994), clearly indicating that uptake via ingested food is the main route of Hg assumption for fish, while uptake via the respiratory system appears less relevant. Specifically, the major contribution derives from the ingestion of polychaetes and decapods, two benthic invertebrates whose dietary preferences include the highly contaminated sediments of the area. From a quantitative viewpoint and in line with experimental results from previous works (Hendriks and Heikens, 2001; Lee and Fisher, 2017; Mackay and Fraser, 2000), the INTFISH model clearly indicates that the ratio between MeHg and Hg^{TOT} in marine organisms strongly increases from phytoplankton (trophic level 1) to fish (trophic level 3), pointing to the fact that the magnitude of MeHg is considerably affected by the structure of respective food web, and confirming that the different contributions to the mercury bio-accumulation along the trophic chain of *M. barbatus* are accurately

Table 3
Comparison between theoretical results and experimental data for each M. barbatus specimen. The percentage of MeHg and IHg obtained by the Integrated Fish Model and the estimated age were also reported.

								Theoretical results		Experimental Data	
Reference	Period	Batch	Fish	Lenght	Estimated Age	MeHg	Hg^{II}	Hg^{TOT}	Av.Hg^{TOT}	Hg^{TOT}	Av.Hg^{TOT}
				mm	months	%	%	$\mu g\,g^{-1}$	$\mu g\,g^{-1}$	$\mu g\,g^{-1}$	$\mu g\,g^{-1}$
			1	200	60	88.7	11.3	1.06		1.06	
Bonsignore et al., 2013	May-12	1	2	168	32	84.5	15.5	0.71	0.94	0.71	0.93
			3	202	63	88.7	11.3	1.06		1.02	
			1	178	39	92	8	2.13			
		1	2	183	43	92.1	7.9	2.29	2.16		2.11
			3	177	38	91.8	8.2	2.07			
Di Bella et al., 2020	Oct-17		1	190	49	91	9	1.67			
		2	2	198	58	91.2	8.8	1.71	1.7		1.7
			3	205	67	91.3	8.7	1.72			

accounted for by the INTFISH model.

INTFISH well reproduces the Hg^{TOT} concentration experimentally measured in the *M. barbatus* specimens caught in the Augusta Bay (Fig. 3; Table 3). The Hg^{TOT} levels in the samples caught in May 2012 ($Hg^{TOT} = 1.06$, 0.71 and 2 and 1.06 $\mu g\,g^{-1}$for fish 1, 2 and 3 respectively) are in very good agreement with the experimental data ($Hg^{TOT} = 1.06$, 0.71 and 1.02 $\mu g\,g^{-1}$ for fish 1, 2 and 3 respectively). The average mercury concentration calculated by the model ($Hg^{TOT} = 0.94\,\mu g\,g^{-1}$) is also very close to that measured experimentally ($Hg^{TOT} = 0.93\,\mu g\,g^{-1}$) in the batch of May 2012. Moreover, the quantitative analysis performed on Hg^{TOT} concentrations in fish collected in October 2017 indicates a good agreement between theoretical results (average $Hg^{TOT} = 2.16$ and 1.70 $\mu g\,g^{-1}$ for batch 1 and 2, respectively) and experimental data (average $Hg^{TOT} = 2.11$ and 1.70 $\mu g\,g^{-1}$for batch 1 and 2, respectively) (Fig. 3; Table 3). The evident matching between numerical simulations and experiments highlights that a major strength of the proposed model is the ability of successfully integrating a set of related models to accurately describe the dynamics of the mercury in the marine species present in a specific contaminated area.

It should be noted that, based on the estimated age (Fig. 3), younger fish (t' < 1 years) have lower Hg content compared with older ones. Overall, from a mathematical viewpoint, the top and bottom panels of Fig. 3 approximately resemble the ideal exponentially converging behaviour expected from a linear model in absence of coupling and time-varying parameters, while the fish trajectory in the middle panel (whose estimated age at capture is the lowest in the May 2012 batch) has still not reached its steady state. Specifically, a substantial increase in Hg^{TOT} concentration is observed between the beginning of stage II (1 < t' < 2 years) and the ending of stage III (2 < t' < 3 years). This is associated with the effect of bioaccumulation, due to the ecological features of the different life stages (Sieli et al., 2011; Fiorentino et al., 2008). In fact, red mullet moves from pelagic (eggs, larvae and juvenile stages) to demersal behaviour (recruitment of juvenile and adult stage). At the end of the first year of the demersal phase, red mullets spread on sandy, muddy and gravely bottoms (Relini et al., 1999; Voliani, 1999), where they usually stay for their remaining lifetime (Voliani, 1999)

4. Conclusions

The INTFISH integrated modelling framework, with its interconnection of modules aiming at quantifying the mercury concentration and accumulation in fish, offers an unprecedented opportunity to track and quantify the dynamics and transient (non-equilibrium) kinetic transfer of Hg from marine sediments and seawater to different levels of the benthic trophic web.

The central module of INTFISH is the Fish model, which analyzes the dynamics of mercury concentration in fish with red mullet (*M. barbatus*) as target species. All stages of fish life cycle are considered, following the time-varying diet preferences of both the red mullet (*M. barbatus*) and its prey. The mercury concentrations in sea water and in first layer of bottom sediments (inputs for the fish respiratory system and for gastro-intestinal tract of mullet prey) are provided by the HR3DHG Model (Denaro et al., 2020), which is coupled in real-time with all the modules of INTFISH.

The integration with the biogeochemical model (which is a key novelty of our approach) allows to take into account the complex dynamics of Hg, and could be particularly interesting in contaminated marine sites where man-made spills of pollutants may undergo variations over time (e.g. seasonal variations) which the model is able to take into consideration, providing a more realistic description of the dynamics involved.

The comprehensive modular structure of INTFISH and its high flexibility in connecting the various steps, capturing the complexity of the biogeochemical structure and reproducing the experimental data, represents a significant step forward towards inclusive and highly performing numerical models, possibly generalizing the setting to trace the fate of mercury and other toxicants from polluted environment in different target species and geographic areas. Based on information related to the diet of a particular human population or of a subgroup with specific characteristics (lifestyle, diet, age range, pregnancy, etc.), the modular structure of the INTFISH model easily allows to shift the attention to different contaminants and/or different polluted sites.

The proposed model, therefore, constitutes a first step of a more ambitious project which aims at providing a quantification of the contaminant intake in the diet of a subject (or a group of subjects) deriving from fish consumption. This would make it possible to evaluate not only the ecological impact of contaminants on the ecosystems but also directly the health risk assessment for humans consuming these resources (Kaikkonen et al., 2020; Senthil Rathi et al., 2021). This will offer an important tool to support decisions for mitigation actions in coastal areas affected by environmental pollution.

Declaration of Competing Interest

The authors declare that they have no known conflicts of interests, competing financial interests or personal relationships that could have influenced the work reported in this paper.

Data availability

The INTFISH model is calibrated and validated using existing experimental data of the Augusta Bay, southern Italy, published in previous papers (Bonsignore et al., 2013; Di Bella et al., 2020).

Acknowledgements

The authors would like to thank Maria Bonsignore, Anna Traina and Mario Sprovieri for fruitful discussions on the topic of the present work. This research has been supported by the Ministry of University, Research and Education of the Italian government under project "Centro

Internazionale di Studi Avanzati su Ambiente, ecosistema e Salute umana – CISAS" (grant no. CUP: B62F15001070005, CIPE n. 105/2015).

References

Alia, A., 2015. Struttura di età del genere Mullus in Alto-Medio Adriatico mediante lettura di otoliti e frequenze di taglia. Tesi di laurea in Biologia delle risorse alieutiche. Alma Mater Studiorum Università di Bologna.

Arnot, J.A., Gobas, F.A., 2004. A food web bioaccumulation model for organic chemicals in aquatic ecosystems. Environ. Toxicol. Chem. 23, 2343–2355.

Ausili, A., Gabellini, M., Cammarata, G., Fattorini, D., Benedetti, M., Pisanelli, B., Gorbi, S., Regoli, F., 2008. Ecotoxicological and human health risk in a petrochemical district of southern Italy. Mar. Environ. Res. 66, 215–217.

Bagnato, E., Sprovieri, M., Barra, M., Bitetto, M., Bonsignore, M., Calabrese, S., et al., 2013. The sea-air exchange of mercury (Hg) in the marine boundary layer of the Augusta basin (southern Italy): concentrations and evasion flux. Chemosphere 93, 2024–2032.

Bellucci, L.G., Giuliani, S., Romano, S., Albertazzi, S., Mugnai, C., Frignani, M., 2012. An integrated approach to the assessment of pollutant delivery chronologies to impacted areas: Hg in the AugustaBay (Italy). Environ. Sci. Technol. 46, 2040–2046.

Beverton, R.J.H., Holt, S.J., 1956. On the dynamics of exploited fish populations. U.K. Min. Agric. Fish., Fish. Invest (Ser. 2) 19, 533p.

Bianchini, M.L., Ragonese, S., 2011. Establishing length-at-age references in the red mullet, *Mullus barbatus* L. 1758 (Pisces, Mullidae), a case study for growth assessments in the Mediterranean Geographical Sub-Areas (GSA). Mediterr. Mar. Sci. 12 (2), 316–332.

Bieser, J., Schrum, C., 2016. Impact of marine mercury cycling on coastal atmospheric mercury concentrations in the North- and Baltic Sea region. Elementa 4, 1–19.

Bizzotto, E., Colombo, F., Pekala, J., Wenning, R.J., Fuchsman, P., 2014. Evaluation of a Conceptual Site Model for Sediment Processes and Geochemical Conditions in a Large Industrial Port Facility (Augusta Bay, Sicily, Italy). Poster.

Bonsignore, M., Salvagio Manta, D., Oliveri, E., Sprovieri, M., Basilone, G., Bonanno, A., et al., 2013. Mercury in fishes from Augusta Bay (southern Italy): risk assessment and health implication. Food Chem. Toxicol. 56, 184–194.

Bonsignore, M., Tamburrino, S., Oliveri, E., Marchetti, A., Durante, C., Berni, A., et al., 2015. Tracing mercury pathways in Augusta Bay (southern Italy) by total concentration and isotope determination. Environ. Pollut. 205, 178–185.

Bonsignore, M., Andolfi, N., Barra, M., Madeddu, M., Tisano, F., Ingallinella, V., Castorina, M., Sprovieri, M., 2016. Assessment of mercury exposure in human populations: a status report from Augusta Bay (southern Italy). Environ. Res. Spec. Issue Hum. Biomonitor. 150, 592–599.

Booth, S., Zeller, D., 2005. Mercury, food webs, and marine mammals: implications of diet and climate change for human health. Environ. Health Perspect. 113 (5), 521–526.

Brender, J.D., Suarez, L., Felkner, M., Gilani, Z., Stinchcomb, D., Moody, K., Henry, J., Hendricks, K., 2006. Maternal exposure to arsenic, cadmium, lead, and mercury and neural tube defects in offspring. Environ. Res. 101 (1), 132–139.

Brunet, C., Casotti, R., Vantrepotte, V., Corato, F., Conversano, F., 2006. Picophytoplankton diversity and photoacclimation in the Strait of Sicily (Mediterranean Sea) in summer. I. Mesoscale variations. Aquat. Microb. Ecol. 44, 127–141.

Brunet, C., Casotti, R., Vantrepotte, V., Conversano, F., 2007. Vertical variability and diel dynamics of picophytoplankton in the Strait of Sicily, Mediterranean Sea, in summer. Mar. Ecol. Prog. Ser. 346, 15–26.

Cadima, E.L., 2003. Fish Stock Assessment Manual. FAO, Fisheries Technical Paper 393. DANIDA, Rome.

Campfens, J., Mackay, D., 1997. Fugacity-based model of PCB bioaccumulation in complex aquatic food webs. Environ. Sci. Technol. 31, 577–583.

Carrier, G., Bouchard, M., Brunet, R.C., Caza, M., 2001. A toxicokinetic model for predicting the tissue distribution and elimination of organic and inorganic mercury following exposure to methyl mercury in animals and humans. II. Application and validation of the model in humans. Toxicol. Appl. Pharmacol. 171, 50–60.

Catalano, D., Ientile, R., Marletta, A., Sciandrello, S., 2014. Monitoraggio Biologico del SIC/ZPS "ITA090014 - Saline di Augusta" e della Foce del Fiume Mulinello nell'Ambito dei Lavori di Ampliamento del Porto Commerciale di Augusta (Terza Fase) – Fase Ante Operam. Relazione Tecnica.

Clark, K.E., Gobas Frank, A.P.C., Mackay, D., 1990. Model of organic chemical uptake and clearance by fish from food and water. Environ. Sci. Technol. 24, 1203–1213.

Connell, D.W., 1990. Bioaccumulation of Xenobiotic Compounds. CRC Press, Boca Raton, FL.

Connolly, J.P., Tonelli, R., 1985. Modelling Kepone in the striped bass food chain of the James River Estuary. Estuar. Coast. Shelf Sci. 20, 349–366.

Cucco, A., Quattrocchi, G., Satta, A., Antognarelli, F., De Biasio, F., Cadau, E., et al., 2016. Predictability of wind induced sea surface transport in coastal areas. J. Geophys. Res. Oceans 121, 5847–5871.

Cucco, A., Quattrocchi, G., Zecchetto, S., 2019. The role of temporal resolution in modeling the wind induced sea surface transport in coastal seas. J. Mar. Syst. 193, 46–58.

De Flora, S., Bennicelli, C., Bagnasco, M., 1994. Genotoxicity of mercury compounds: a review. Mutat. Res. 317, 57–79.

De Marchis, M., Freni, G., Napoli, E., 2014. Three-dimensional numerical simulations on wind- and tide-induced currents: the case of Augusta harbour (Italy). Comput. Geosci. 72, 65–75.

Denaro, G., Salvagio Manta, D., Borri, A., Monsignore, M., Valenti, D., Quinci, E., et al., 2020. HR3DHG version 1: modelling the spatio-temporal dynamics of mercury in the Augusta Bay (southern Italy). Geosci. Model Dev. 13, 1–21.

Di Bella, C., Traina, A., Giosué, C., Carpentieri, C., Lo Dico, G.M., Bellante, A., Del Core, M., Falco, F., Gherardi, S., Uccello, M.M., Ferrantelli, V., 2020. Heavy metals and PAHs in meat, milk and seafood from Augusta area (Southern Italy): contamination levels, dietary intake, and human exposure assessment. Front. Public Health 8. Article 273.

Esposito, V., Andaloro, F., Bianca, D., Natalotto, A., Romeo, T., Scotti, G., Castriota, L., 2014. Diet and prey selectivity of the red mullet, Mullus barbatus (Pisces: Mullidae), from the southern Tyrrhenian Sea: the role of the surf zone as a feeding ground. Mar. Biol. Res. 10 (2), 167–178.

Fauchald, K., Jumars, P.A., 1979. The diet of worms: a study of polychaete feeding guilds. Oceanogr. Mar. Biol. Annu. Rev. 17, 193–284.

Synthesis of information on some target species in the MedSudMed Project area (central Mediterranean). GCP/RER/010/ITA/MSM-TD-15. In: Fiorentino, F., Ben Meriem, S., Bahri, T., Camilleri, M., Dimech, M., Ezzeddine-Naja, S., Massa, F., Jarboui, O., Zgozi, S. (Eds.), MedSudMed Technical Documents 15, 67.

Fitzgerald, W.F., Lamborg, C.H., Hammerschmidt, C.R., 2007. Marine biogeochemical cycling of mercury. Chem. Rev. 107 (2), 641–662.

Gobas, F.A., MacKay, D., 1987. Dynamics of hydrophobic organic chemical bioconcentration in fish. Environ. Toxicol. Chem. Int. J. 6 (7), 495–504.

Gworek, B., Bemowska-Kałabun, O., Kijeńska, M., Wrzosek-Jakubowska, J., 2016. Mercury in marine and oceanic waters - a review. Water Air Soil Pollut. 227–371.

Hamelink, J.L., Waybrant, R.C., Ball, R.C., 1971. A proposal: exchange equilibria control the degree chlorinated hydrocarbons are biologically magnified in lentic environments. Trans. Am. Fish. Soc. 100, 207–214.

Harding, G., Dalziel, J., Vass, P., 2018. Bioaccumulation of methylmercury within the marine food web of the outer Bay of Fundy, Gulf of Maine. PLoS One 13 (7), e0197220.

He, W., Qin, N., He, Q.-S., Wang, Y., Kong, X.Z., Xu, F.-L., 2012. Characterization, ecological and health risks of DDTs and HCHs in water from a large shallow Chinese lake. Ecol. Inform. 12, 77–84.

Hendriks, A.J., 1995. Modelling non-equilibrium concentrations of microcontaminants in organisms: comparative kinetics as a function of species size and octanol-water partitioning. Chemosphere 30 (2), 265–292.

Hendriks, A.J., 1999. Allometric scaling of rate, age and density parameters in ecological models. Oikos 86, 293–310.

Hendriks, A.J., Heikens, A., 2001. The power of size. 2. Rate constants and equilibrium ratios for accumulation of inorganic substances related to species weight. Environ. Toxicol. Chem. 20 (7), 1421–1437.

Hendriks, A.J., Van der Linde, A., Cornelissen, G., Sijm, D.T.H.M., 2001. The power of size. 1. Rate constants and equilibrium ratios for accumulation of organic substances related to octanol-water partition ratio and species weight. Environ. Toxicol. Chem. 20 (7), 1399–1420.

Hylander, L.D., Goodsite, M.E., 2006. Environmental costs of mercury pollution. Sci. Total Environ. 368 (1), 352–370.

ICRAM, 2008. Progetto preliminare di bonifica dei fondali della rada di Augusta nel sito di interesse nazionale di Priolo e Elaborazione definitiva, BoI-Pr-SI-PR-Rada di Augusta-03.22.

Jagadeep, C.S., Chandana, G.L., Naganagouda, V.K., Sharath, C., 2020. Recent scenario of impact of xenobiotics on marine fish: an overview. Pharm. J. 12 (6), 1797–1800.

Jin, L., Liu, M., Zhang, L., Li, Z., Yu, J., Liu, J., Ye, R., Chen, L., Ren, A., 2016. Exposure of methyl mercury in utero and the risk of neural tube defects in a Chinese population. Reprod. Toxicol. 61, 131–135.

Johnsson, C., Schütz, A., Sällsten, G., 2005. Impact of consumption of freshwater fish on mercury levels in hair, blood, urine, and alveolar air. J. Toxic. Environ. Health A 68 (2), 129–140.

Kaikkonen, L., Parviainen, T., Rahikainen, M., Uusitalo, L., Lehikoinen, A., 2020. Bayesian networks in environmental risk assessment: a review. Integr. Environ. Assess. Manag. 17 (1), 62–78.

Kobayashi, Y., Yoshida, K., 2021. Development of QSAR models for prediction of fish bioconcentration factors using physicochemical properties and molecular descriptors with machine learning algorithms. Ecol. Inform. 63, 101285.

Kütter, V.T., Mirlean, N., Baisch, P.R.M., Kütter, M.T., Silva-Filho, E.V., 2009. Mercury in freshwater, estuarine, and marine fishes from Southern Brazil and its ecological implication. Environ. Monit. Assess. 159, 35.

La Colla, N.S., Botté, S.E., Marcovecchio, J.E., 2019. Mercury cycling and bioaccumulation in a changing coastal system: from water to aquatic organisms. Mar. Pollut. Bull. 140, 40–50.

Law, F.C.P., Abedini, S., Kennedy, C.J., 1991. A biologically based toxicokinetic model for pyrene in rainbow trout. Toxicol. Appl. Pharmacol. 110, 390–402.

Le Donne, K., Ciafani, S., 2008. Monitoraggio dell'inquinamento atmosferico da mercurio nei principali impianti cloro-soda italiani. Ing. Ambient. 37, 45–52.

Lee, C.S., Fisher, N.S., 2017. Bioaccumulation of methylmercury in a marine copepod. Environ. Toxicol. Chem. 36, 1287–1293.

Leonard, D., Reash, R., Porcella, D., Paralkar, A., Summers, K., Gherini, S., 1995. Use of the mercury cycling model (MCM) to predict the fate of mercury in the Great Lakes. Water Air Soil Pollut. 80, 519–528.

Li, M.L., Gillies, E.J., Briner, R., Hoover, C.A., Sora, K.J., Loseto, L.L., Walters, W.J., Cheungd, W.W.L., Giang, A., 2022. Investigating the dynamics of methylmercury bioaccumulation in the Beaufort Sea shelf food web: a modeling perspective. Environ Sci Process Impacts 24, 1010.

Likens, G.E. (Ed.), 2009. Encyclopedia of Inland Waters. Elsevier.

Mackay, D., 1982. Correlation of bioconcentration factors. Environ. Sci. Technol. 16, 274–278.

Mackay, D., Fraser, A., 2000. Bioaccumulation of persistent organic chemicals: mechanisms and models. Environ. Pollut. 110, 375–391.
Mahmood, M., Bhavsar, S.P., Arhonditsis, G.B., 2013. Fish contamination in Lake Erie: an examination of temporal trends of organochlorine contaminants and a Bayesian approach to consumption advisories. Ecol. Inform. 18, 131–148.
Marziali, L., Roscioli, C., Valsecchi, L., 2021. Mercury bioaccumulation in benthic invertebrates: from riverine sediments to higher trophic levels. Toxics 9, 197.
Massel, S.R., 1999. Fluid Mechanics for Marine Ecologists. Springer- Verlag, Berlin Heidelberg, 1999.
Matsumoto, H., Koya, G., Takeuchi, T., 1965. Fetal Minamata disease: a neuropathological study of two cases of intrauterine intoxication by a methyl mercury compound. J. Neuropathol. Exp. Neurol. 24 (4), 563–574.
McKinney, R.A., Glatt, S.M., Williams, S.R., 2004. Allometric length-weight relationships for benthic prey of aquatic wildlife in coastal marine habitats. Wildl. Biol. 10 (1), 241–249.
Mergler, D., Anderson, H.A., Hing Man Chan, L., Mahaey, K.R., Murray, M., Sakamoto, M., Stern, A.H., 2007. Methylmercury exposure and health effects in humans: a worldwide concern. AMBIO 36 (1), 3–11.
Morcillo, P., Esteban, M.A., Cuesta, A., 2017. Mercury and its toxic effects on fish. AIMS Environ. Sci. 4 (3), 386–402.
Neely, W.B., Branson, D.R., Blau, G.E., 1974. Partition coefficients to measure bioconcentration potential of organic chemicals in fish. Environ. Sci. Technol. 8, 1113–1115.
Ni, F.J., Arhonditsis, G.B., 2023. Examination of the effects of toxicity and nutrition on a two prey-predator system with a metabolomics-inspired model. Ecol. Inform. 101905.
Ni, F.J., Kelly, N.E., Arhonditsis, G.B., 2017. Towards the development of an ecophysiological Daphnia model to examine effects of toxicity and nutrition. Ecol. Inform. 41, 91–107.
Nichols, J.W., McKim, J.M., Andersen, M.E., Gargas, M.L., Clewell III, H.J., Erickson, R. J., 1990. A physiology based toxicokinetic model for the uptake and disposition of waterborne organic chemicals in fish. Toxicol. Appl. Pharmacol. 106, 433–447.
Oliveri, E., Salvagio Manta, D.S., Bonsignore, M., Cappello, S., Tranchida, G., Bagnato, E., et al., 2016. Mobility of mercury in contaminated marine sediments: biogeochemical pathways. Mar. Chem. 186, 1–10.
Pipitone, C., Arculeo, M., 2003. The marine Crustacea Decapoda of Sicily (Central Mediterranean Sea): a checklist with remarks on their distribution. Ital. J. Zool. 70, 69–78.
Radomyski, A., Ciffroy, P., 2015a. The Phytoplankton MERLIN-Expo Model, Fun Project 4 - Seventh Framework Programme.
Radomyski, A., Ciffroy, P., 2015b. The Invertebrate MERLIN-Expo Model, Fun Project 4 - Seventh Framework Programme.
Radomyski, A., Ciffroy, P., 2015c. The Fish MERLIN-Expo Model, Fun Project 4 - Seventh Framework Programme.
Relini, G., Bertrand, J., Zamboni, A., 1999. Sintesi delle conoscenze sulle risorse da pesca dei fondi del Mediterraneo centrale (Italia e Corsica). Biol. Mar. Medit. 6 (suppl. 1), 868.
Sadutto, D., Andreu, V., Ilo, T., Akkanen, J., Picó, Y., 2021. Pharmaceuticals and personal care products in a Mediterranean coastal wetland: impact of anthropogenic and spatial factors and environmental risk assessment. Environ. Pollut. 271.
Salvagio Manta, D., Bonsignore, M., Oliveri, E., Barra, M., Tranchida, G., Giaramita, L., et al., 2016. Fluxes and the mass balance of mercury in Augusta Bay (Sicily, southern Italy). Estuar. Coast. Shelf S 181, 134–143.
Schmidt, T.M. (Ed.), 2019. Encyclopedia of Microbiology. Academic Press.
Senthil Rathi, B., Senthil Kumar, P., Vo, Dai-Viet N., 2021. Critical review on hazardous pollutants in water environment: occurrence, monitoring, fate, removal technologies and risk assessment. Sci. Total Environ. 797.
Sharpe, S., Mackay, D., 2000. A framework for evaluating bioaccumulation in food webs. Environ. Sci. Technol. 34 (12), 2373–2379.
Sieli, G., Badalucco, C., Di Stefano, G., Rizzo, P., D'Anna, G., Fiorentino, F., 2011. Biology of red mullet, Mullus barbatus (L. 1758), in the Gulf of Castellammare (NW Sicily, Mediterranean Sea) subject to a trawling ban. J. Appl. Ichthyol. 27 (5), 1218–1225.
Signa, G., Mazzola, A., Tramati, C.D., Vizzini, S., 2017. Diet and habitat use influence Hg and Cd transfer to fish and consequent biomagnification in a highly contaminated area: Augusta Bay (Mediterranean Sea). Environ. Pollut. 230, 394–404.
Sprovieri, M., Oliveri, E., Di Leonardo, R., Romano, E., Ausili, A., Gabellini, M., et al., 2011. The key role played by the Augusta basin (southern Italy) in the mercury contamination of the Mediterranean Sea. J. Environ. Monit. 13, 1753–1760.
Stockner, J.G., Antia, N.J., 1986. Algal picoplankton from marine and freshwater ecosystems: a multidisciplinary perspective. Can. J. Fish. Aquat. Sci. 43 (12), 2472–2503.
Storelli, M.M., Giacominelli Stuffler, R., Storelli, A., Marcotrigiano, G.O., 2003. Total and methylmercury content in edible fish from the Mediterranean Sea. J. Food Prot. 66, 300–303.
Storelli, M.M., Storelli, A., Giacominelli-Stuffler, R., Marcotrigiano, G.O., 2005. Mercury speciation in the muscle of two commercially important fish, hake (*Merluccius merluccius*) and striped mullet (*Mullus barbatus*) from the Mediterranean Sea: estimated weekly intake. Food Chem. 89, 295–300.
Strickland, J.D.H., 1960. Measuring the Production of Marine Phytoplankton. Fisheries Research Board of Canada (Bulletin).
Thomann, R.V., 1981. Equilibrium model of fate of microcontaminants in diverse aquatic food chains. Can. J. Fish. Aquat. Sci. 38 (3), 280–296.
Thomann, R.V., 1989. Bioaccumulation model of organic chemical distribution in aquatic food chains. Environ. Sci. Technol. 23, 699–707.
Thomann, R.V., Connolly, J.P., 1984. Model of PCB in the Lake Michigan lake trout food chain. Environ. Sci. Technol. 18, 65–71.
Tursi, A., Matarrese, A., D'Onghia, G., Sion, L., Maiorano, P., 1996. The yield per recruit assessment of hake (*Merluccius merluccius* L. 1758) and red mullet (*Mullus barbatus* L. 1758) in the Ionian Sea. FAO Fish. Rep. 533, 127–141.
Umgiesser, G., 2009. SHYFEM, Finite Element Model for Coastal Seas. User Manual. The SHYFEM Group, Georg Umgiesser, ISMAR-CNR, Venezia, Italy.
Umgiesser, G., Ferrarin, C., Cucco, A., De Pascalis, F., Bellafiore, D., Ghezzo, M., et al., 2014. Comparative hydrodynamics of 10 Mediterranean lagoons by means of numerical modelling. J. Geophys. Res. Oceans 119, 2212–2226.
Van der Oost, R., Beyer, J., Vermeulen, N.P.E., 2003. Fish bioaccumulation and biomarkers in environmental risk assessment: a review. Environ. Toxicol. Pharmacol. 13 (2), 57–149.
Veith, G.D., Defoe, D.L., Bergstedt, B.V., 1979. Measuring and estimating the bioconcentration factor of chemicals in fish. J. Fish. Res. Board Can. 36, 1040–1048.
Visha, A., Lau, A., Yang, C., Bhavsar, S.P., Depew, D., Matos, L., Ni, F., Arhonditsis, G.B., 2021. A probabilistic assessment of the impairment status of areas of concern in the Laurentian Great Lakes: how far are we from delisting the Hamilton harbour, Lake Ontario, Canada? Ecol. Inform. 62, 101271.
Voliani, A., 1999. Mullus barbatus. In: Synthesis of knowledge on bottom fishery resources in central mediterranean (Italy and Corsica). G. Relini, J. Bertrand and A. Zamboni (Eds). Biol. Mar. Medit. 6 (Suppl. 1), 276–291.
Von Bertalanffy, L., 1934. Untersuchungen über die Gesetzlichkeit des Wachstums. I. Allgemeine Grundlagen der Theorie; mathematische und physiologische Gesetzlichkeiten des Wachstums bei Wassertieren. Archiv für Entwicklungsmechanik 131, 613–652.
Von Bertalanffy, L., 1938. A quantitative theory of organic growth. Hum. Biol. 10 (2), 181–213.
Von Bertalanffy, L., 1949. Problems of organic growth. Nature 163, 156–158.
Von Bertalanffy, L., 1957. Quantitative laws in metabolism and growth. Q. Rev. Biol. 32, 217–231.
Watras, C., Bloom, N.S., 1994. The vertical distribution of mercury species in Wisconsin Lake: accumulation in plankton layers. Limnol. Libr. 37–152.
Yakovlev, V.A., Yakovleva, A.V., 2010. Polychaete *Hypania invalida* (Polychaeta: Ampharetidae) in the Kuybyshev reservoir: distribution and size and weight parameters. Russ. J. Biol. Invasions 1 (2), 145–151.